ADDIS ABABA UNIVERSITY

SCHOOL OF GRADUATE STUDIES

ADDIS ABABA INSTITUTE OF TECHNOLOGY

SCHOOL OF ELECTRICAL AND COMPUTER ENGINEERING

MODELING, DESIGN AND CONTROL OF THE BELT DRIVE SYSTEM IN FINCHAWA SUGAR FACTORY

By

Deressa Tesfaye

Advisor

Dr. Dereje Shiferaw.

A Thesis Submitted to the School of Graduate Studies of Addis Ababa University in Partial Fulfillment of the Requirements for the Degree of

Masters of Science in Electrical and computer Engineering

Stream: - Control Engineering

December, 2017

Addis Ababa, Ethiopia

ADDIS ABABA UNIVERSITY

SCHOOL OF GRADUATE STUDIES

ADDIS ABABA INSTITUTE OF TECHNOLOGY

SCHOOL OF ELECTRICAL AND COMPUTER ENGINEERING

MODELING, DESIGN AND CONTROL OF THE BELT DRIVE SYSTEM

IN FINCHAWA SUGAR FACTORY

By

Deressa Tesfaye

Approved by the Board of Examiners:

_____	_____
Advisor	Signature
_____	_____
Internal Examiner	Signature
_____	_____
External Examiner	Signature

Declaration

I, the undersigned, declare that this MSc thesis comprises my own work. I have dually acknowledged and referenced all materials used in this work. I understand that non-adherence to the principle of academic honesty and integrity, misrepresentation/fabrication of any idea/data/fact/source will constitute sufficient ground for disciplinary action by the university and can also evoke penal action from the source which have not been properly cited or acknowledged.

Signature _____

Deressa Tesfaye

Date _____

This thesis work has been submitted for examination with my approval as a University advisor.

Advisor's Name Signature

_____

Dr. Dereje Shiferaw

ACKNOWLEDGEMENT

First and for most, my thanks goes to Almighty God for his kindly provision of wisdom and inspiration required for the successful completion of this paper.

Next to God I would like to forward my sincere gratitude to my advisor **Dr. Dereje Shiferaw** for his unreserved effort in bringing this thesis work to reality. I am in a position where I cannot take the sole credit for the completion of this study. I credit every piece of strength of this study to my advisor and any weakness to myself.

I also owe a great deal of gratitude to my family and my friends for their moral support.

ABSTRACT

This thesis presents the modeling, design and control of the belt drive system in Finchawa sugar factory.

Belt drives have been serving in this industry for a long period of time. Certain features of belt drives such as slippage, tension fluctuations, and sliding of the belt on the pulleys lead to highly nonlinear deformation, large rigid body motion, dynamical contact with sticking and slipping zones and cyclic tension. In addition to these problems, in Finchawa sugar factory, the tracking control mechanism of the belt drive system has many problems. The main problem is slow response and lack of accuracy. This is because the control is manual with simple ON/OFF control mechanism which is more difficult to obtain fast response and accurate tracking.

The performance of motion control for belt drives is important in many industrial fields and is affected by these factors. PI control can improve performance specification of belt drive system and result in a faster dynamic response and more accuracy.

Hence in this thesis, modeling of a linear belt-drive system and designing of PI controller for its position and speed control mechanisms has been examined by *changing the reference of the system with the maximum steady state error of 0.0027% and good transient performance with rise time less than 0.1 second.*

Friction phenomena and position dependent elasticity of the belt was analyzed. The PI controller has been designed for accurate speed and position control mechanism and was simulated on MATLAB.

Keywords: Belt-drive system, nonlinearities modeling, tracking control, PI control.

Contents

LIST OF TABLES AND LIST OF FIGURES

List of table

List of figures

ABBREVIATIONS AND SYMBOLS

A/D	Analog to Digital
AC	Alternating Current
BLDC	Brushless Direct Current
DC	Direct Current
EMF	Electromotive Force
LED	Light Emitting Diode
LVDT	Linear Variable Differential Transformer
PI	Proportional-Integral
PM	Permanent Magnet
PMSM	Permanent Magnet Synchronous Machine
PWM	Pulse Width Modulation
Φ	Magnetic flux
δ	Empirical parameter in friction model
ε	Relative elongation
θ	Actual position
ρ	Mass per unit volume
τ	Torque produced by motor
$\tau f1, \tau f2$	Friction torques in the pulleys
τref	Torque reference
φ	Angular position of motor shaft
ωr	Actual rotor speed
ωset	Speed error
ωref	Reference speed signal

CHAPTER ONE

INTRODUCTION

1.1 Background

The belt drives are currently a popular form of material transportation. They have been used in industry for over 200 years and have played an important role in the industrial revolution. Belt drives are widely used in different fields of human activity to transmit the mechanical energy from the rotating shaft to the objects of the control. In industry such drives can be used for objects control positioning and transportation [3].

Historically belt system has been used to transmit power at up to 98% efficiency between rotational machine elements. Typical application for such system is a conveyor, the first prototype of which has been used since 19th century.

In [4], the belt drive systems are widely spread in automotive industry and in conveyor type application. Ford introduced the first conveyor belt-based assembly line in Ford Motor Company's factory. Motion control requirements for such system are accurate velocity control, linear motion and high resolution.

Using of belt for high precision applications has become appropriate because of rapid development of motor and drive technology as well as the implementation of timing belts in belt-driven systems. Toothed or timing belts with correct tension exclude slippage and increase the precision of motion. As a result, the use of belts in drives has caused a number of advantages. Systems can provide high speed and acceleration, accurate and repeatable motion, high efficiency, long stroke lengths and low cost [2].

Nowadays, the study of the belt drive system mechanics and dynamics have been merged together to create a more accurate model for control design [7].

1.2 PROBLEM STATEMENT

During my internship program the problem what I have observed in Finchawa sugar factory was there is the speed and position control mechanism of the belt drive system which feeds the bagasse to the boiler combustion system. Boiler also known as the heart of Factory which uses the byproduct of the factory bagasse as fuel, water and heated air to produces 65 tons of dry steam with 25-30bar pressure per hour. The liberated from the fuel is used to convert the water pumped through the water tubes to dry steam.

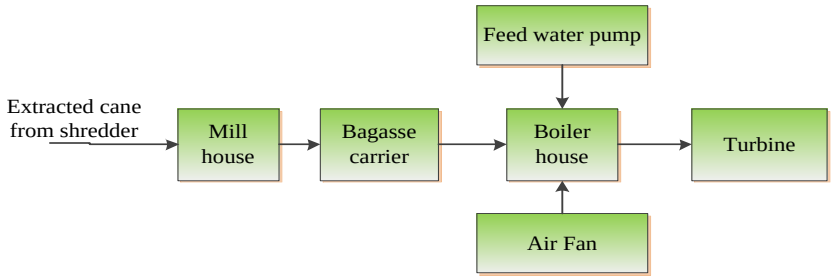

Figure 1.1 Belt drive system description in Finchawa Sugar Factory from mill house to boiler house

The company uses the speed and position control mechanism for the belt drive system to transport the bagasse in between the mill house and the boiler is the manual one with simple ON/OFF control mechanism. In this case both the position and speed of the belt system is not well controlled. Most of the time when the bagasse is transported from the mill house to the boiler house there is some piece biomass failed to the ground from the bagasse carrier due to the lack of accuracy of the belt drive system position control mechanism. And also after the juice is extracted from the cane the bagasse will travel to the boiler. This bagasse is a common fuel sources for the boiler with the constant amount. But the speed of the bagasse carrier belt is not constant due to the lack control mechanism. Not only this, the friction phenomena and position dependent elasticity of the belt may lead the belt drive system to nonlinear deformation. In general the mechanism they use to control this belt drive system is not good to meet the required specifications.

1.3. Objectives of the thesis

1.3.1. General Objective:

The research work is aimed at:

- Modeling, design and control of the belt drive system in Finchawa sugar factory.

1.3.2. Specific Objectives:

The specific objectives of this work are:

- To model and simulate the belt drive system in Finchawa sugar factory in order to analyze its performance.
- To design a PI controller for accurate speed and position control of belt drive system.
- To analyze the performance of PI controller for tracking control of belt drive system in both speed and position control mechanism.

1.4 Methodology

The modeling and design of tracking control for belt drive system is shown in Figure 1.1. In this thesis work, PI control based on the closed loop speed control for the general belt drive system has been designed and mathematically modeled and also the requirements of motion control system in Finchawa sugar factory has been explained. The PI controller was designed for accurate speed control and accurate position control and was simulated on MATLAB Simulink. The data required for the study was identified and collected by literature survey and MATLAB simulation.

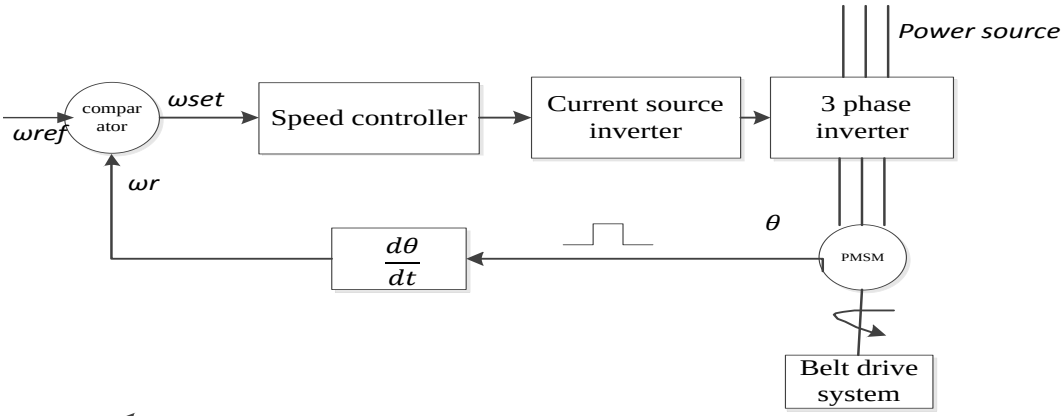

Figure 1.2 General block diagram of the system

Fig. 1.1 represents a standard scheme of servo drive system. The servo control is based on a cascade principle, where the speed reference for the speed controller is fed by higher-level controller. The speed error ωset, which is the difference between the reference signal ωref and the actual rotor speed ωr is measured by a speed sensor and go through the speed controller that produces the reference signal for the current source inverter. The current source inverter produces the output signal, which is amplified by the three phase inverter feeding voltage to the motor phases.

1.5. Literature Overview

Considerable research has been performed on the control of belt-drives in recent years.

Li and Cheng (1994) presented a PID controller with adaptive compensation of inertial force for a belt-driven high speed positioning table. Li and Rehani (1996) designed a PID controller with acceleration and Coulomb friction compensation (PIDAF) for the tracking control of the angular position of the belt drive turning table based on an identified model. Lee and Rutherford (1999) presented the frequency reshaped linear quadratic (FRLQ) control in the development of a low-cost human level performance belt driven robot. In their work, a simple first order filter was chosen for determining a performance index for the linear quadratic optimal controller that would panelize the frequencies at or above the first resonance frequency of the belt drive. Jayewardene, Nakamura and Goto (2003) presented a PID control algorithm with an off line trajectory planning under maximum velocity and acceleration constraints with compensation of delay dynamics and vibrations for accurate position control of belt drives. The same strategy was utilized for the cooperative control of two industrial robots and belt drive machines (Jayewardene, 2009). Selezneva (2009) implemented a PID algorithm with automatic tuning for the tracking control of the belt-drive systems. Among those control algorithms mentioned above, the PID controllers are widely used in the process industries and commercial controller hardware. It is also used in a non-model based friction compensation, which can eliminate stick-slip in high-stiffness system.

1.6 Outline of the thesis

To meet the above objectives, this thesis is organized as follows: In chapter 2 the linear belt drive system and its application will be provided and also the requirements of motion control system in Finchawa sugar factory were explained. Modeling of the general belt drive system and the description of the over whole system was also described in chapter 3. And also the general control mechanism of the belt drive system was presented in chapter 3. The simulation and discussion results were presented in chapter 4. Conclusions on the performance of the controllers are provided in chapter 5.

CHAPTER TWO

REQUIREMENTS OF MOTION CONTROL SYSTEMS IN FINCHAWA SUGAR FACTORY AND MOTOR SELECTION

2.1. Requirements of motion control systems in Finchawa sugar factory

The object of attention in this work is servo drives. The term "servo" in context of motors and drives means that they are used for the position control. [3] An electrical servo system includes four main parts: a servomotor, a power converter, sensors and a load. Modern closed-loop control systems allow the servo drives to achieve high dynamic performance with high efficiency. [4]The modern servo systems are characterized by the strong requirements for the next important properties:

- ✓ Positioning accuracy
- ✓ Speed accuracy
- ✓ torque stability
- ✓ overload capability
- ✓ dynamic performance

The typical applications for servo drives are robots, transfer lines, conveyors, and lifts and coordinate measuring systems [5].

In spite of the wide spread occurrence of electrical motors, the precision requirements for servo drives constantly increase [7].

A typical servo drive consists of four main parts. One of the important belt drive design decisions that should be taken into account is the motor selection. There are many available alternatives; each of them will have benefits and disadvantages. Considering the whole servo system the motor determines the characteristics of drive and it also determines the power converter and control requirements. [6] Many possibilities exist but only limited number will have enough broad characteristics, which are required for the precise motion control with the requirements of machine tool drive:

- ✓ A high speed-to-torque ratio
- ✓ Four-quadrant application

- ✓ The ability to produce a torque at a standstill
- ✓ A high power-to-weight ratio
- ✓ High system reliability

The following motor types can satisfy the criteria listed above and they are widely used in servo systems:

- ✓ brushed DC motors
- ✓ brushless DC motors
- ✓ permanent magnet synchronous motors (PMSMs)
- ✓ induction motors
- ✓ stepper motors
- ✓ linear motors

2.2. Common motor types and motor selection criteria in belt drive system motion control

The first speed-controlled drive was introduced by Harry Ward Leonard and it required three machines for scheme implementation. After the invention of transistor and rapid development of electronics, new possibilities for accurate control of DC motor, such as PWM technology appeared. Brushless DC motors with permanent magnets were introduced in early 1960s, but their power was limited due to not enough powerful PM materials. Brushless DC motors for higher power application became available only after the invention of PM materials with high energy density in the beginning of 1980s. Later on, when the field-oriented control was introduced, it was possible to apply AC motors for speed-controlled applications. First speed-controlled AC drives were induction motors but in early 1990s the vector control was also developed for PMSMs. Also, with rapid development of computer science became accessible control of stepper motors directly from microcontrollers. All these motor types are available for wide range of motion control applications. The most common of them are considered below in more detailed.

Brushed DC motors

DC machine was the first practical device, which converts electrical power into the mechanical and vice versa in its generator mode. The simplest example of the DC motor is shown in Fig.2.1.In this case, the stationary magnetic flux Φ is produced by poles and when voltage is applied on the brushes, current flows through the armature and generates force *f* which forms torque and causes the armature to rotate.

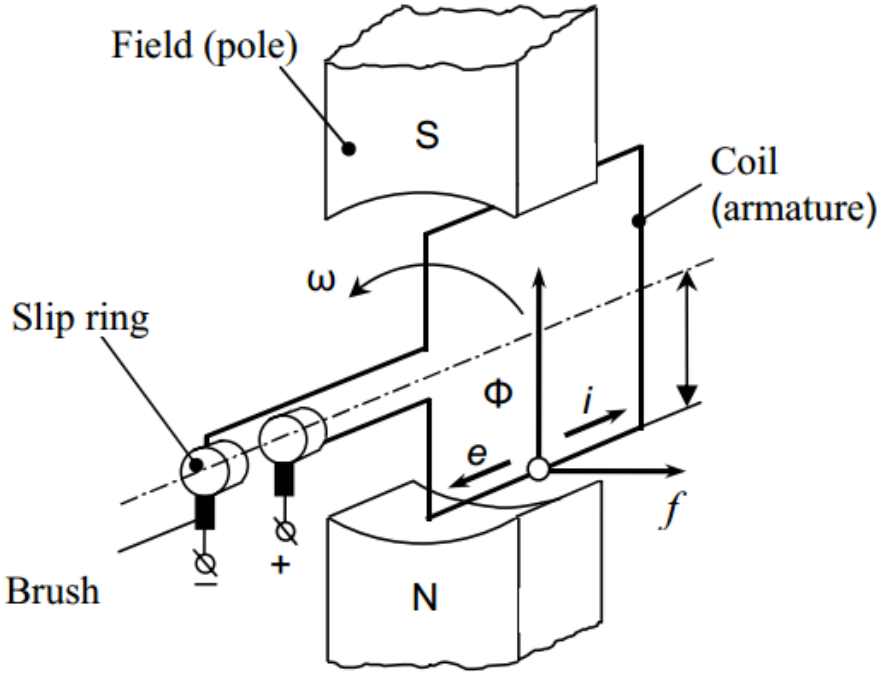

Figure.2.1. Elementary DC motor [9]

The reasons for widespread expansion of the DC motor in many types of industrial drive applications are good control characteristics (speed versus voltage and speed versus torque), good performance and high efficiency. In spite of rapid development of the lower-cost motors, advantages associated with inherent stability and relatively simple control of DC machine, are indisputable. In separately excited DC motors torque and thus also the speed can be controlled by armature current by adjusting the armature voltage. The field can be controlled by adjusting the excitation current of the separate magnetizing winding.

The flux and torque are therefore separately controllable. On this basic principle was built thyristor control for higher-power rating of drives used for printing and paper industry and

chopper control for lower-power applications. Development in permanent magnet materials led to invention of permanent magnet DC motors (PMDC), in which the stator excitation windings were replaced by permanent magnets. Reasons for using PMDC are extremely linear speed-torque characteristics, small torque ripple at low speeds, absence of copper losses in excitation windings and small rotor diameter.

The characteristics of the DC motors are not ideal for applications with strict requirements for reliability, service interval and noises due to the mechanical and electrical limits set by the motor commutator. In addition, the carbon brushes require regular service.

The other drawback of the DC motors is the fact that while the rotation speed increases, the voltage between commutator segments also increases and in combination with high armature current, a voltage breakdown between adjacent commutator segments will result in motor brush fire or flashover. It should be avoided since it damages the commutator and brush gear and reduces the life expectancy of the motor. Thus operational area of the motor is bounded by different factors. Despite these disadvantages numerous applications require drives based on brushed DC motors. In spite of the good control characteristics enumerated drawbacks of DC motors are inconvenient for producing reliable high-performance belt drives.

Induction motors

The AC squirrel-cage induction motors are the largest group of all electrical drives in the industry. It has been estimated that they are used in 70-80% of all industrial drive applications, especially in fixed-speed applications such as pump or fan drives. The benefits of induction motor are undisputable: simple construction, low cost compared to other motors, simple maintenance, high efficiency and satisfactory characteristics at the high speeds. With appropriate power electronics converters induction motors are used in wide power range from kW to MW levels.

A common structure of induction motor is represented in Fig.1.4. Stator rotation field induces an electromotive force in the short-circuited rotor winding. Due to the induced voltage and short-circuited winding, current occurs in the rotor and electromagnetic torque is produced.

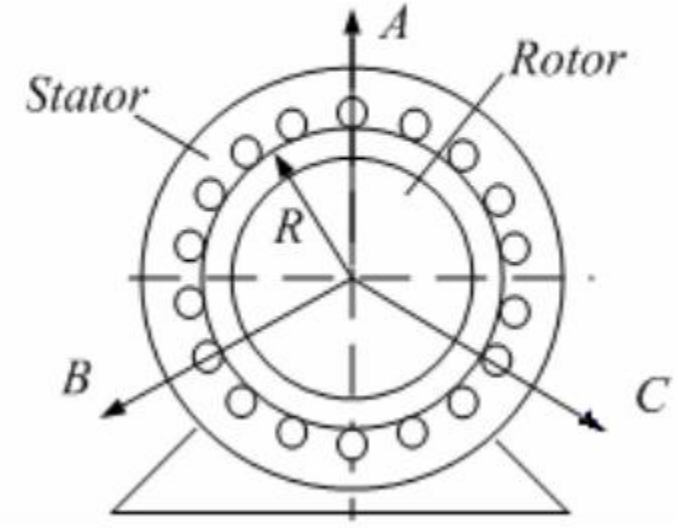

Figure 2.2 Common structure of induction machine.

Induction motor was invented in the end of 19th century. Its theory is well-known and power electronic converter technology provides appropriate variable-voltage/current, variable-frequency supply for efficient and stable variable-speed control. Thus, it is possible to obtain a dynamic performance in all respects better than which could be obtained with a phase-controlled DC drive combination. The significant characteristic of the induction motor is a slip caused by the rotor lagging the rotating stator magnetic field.

Rotor copper losses are directly proportional to the slip. For example, the rotor copper losses in 4 kW motor are approximately 4.7% of the nominal power if the efficiency of 85% is supposed [10].The slip has also impact when a high dynamic performance is needed, since it de rates the transient response of the motor.

The main disadvantage of the induction motor for the servo control systems is the non-linear speed versus torque and speed versus control voltage characteristics. Therefore such motors are inconvenient for the implementation of the belt-drives.

Brushless DC motors

An impetus to the recent development of brushless DC motors was given by computer-peripheral and aerospace industries, where high performance coupled with reliability and low maintenance are essential. [3] Typically, the brushless DC motor has a three-phase stator, and the rotor has surface-mounted magnets that create rectangular air gap flux distribution. The motor is driven by rectangular or trapezoidal voltage pulses paired with the given rotor position. In order to generate the maximum torque, the angle between the stator flux and the rotor flux must be kept close to 90°. The position sensor required for the commutation can be rather simple, because only the relative orientation of the rotor to the stator coils is needed. Typically, simple Hall Effect sensors or low resolution optical encoders are sufficient. Figure 2.3 represents the geometry of BLDC motor and the stator current and back-EMF waveforms.

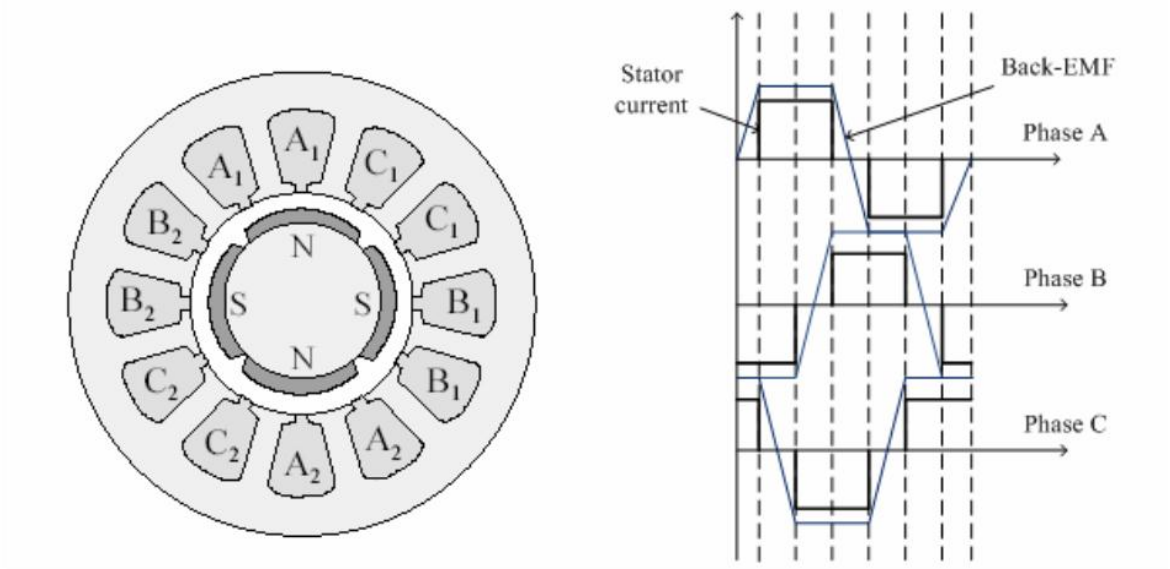

Figure 2.3. the geometry and the operating principle of the BLDC motor: a) four-pole brushless DC motor; b) phase-current and back-EMF waveforms in ideal case. [8]

Nowadays, the industrial applications of brushless DC motors have developed thanks to several reasons, namely: reduction of price of power conversion equipment, creation of advanced control schemes for PWM inverters, development of new more powerful magnetic materials, development of highly accurate position controllers and manufacturing and integration of all

these components in compact size. Moreover, they are easy to control because the torque is generated in proportion to the current.

Comparison of the brushless DC motor with the brushed DC motor shows that the BLDC motor has a number of advantages. Firstly, the construction of the motor allows direct heat dissipation to the environment without heat flow through the air gap and bearings.

Therefore additional cooling system is not usually required. Secondly, brushless DC motors provide more accurate overload protection, because the temperature of the hottest part can be detected directly [5]. In addition, some advantages are connected with absence of mechanical commutator:

- ✓ There is no sparking; that is the motor can be used in hazardous environments.
- ✓ Maintenance costs are reduced; brushless DC motors do not require regular service of the brush gear.
- ✓ The speed-torque limits caused by commutator are eliminated.

However, benefits rarely exist without disadvantages. In brushless DC motor the mechanical commutator is replaced by an electronic system including a three- (or two-) phase power bridge, a rotor position encoder with a proper resolution and commutator logic to switch the bridge's semiconductor devices in a correct sequence to generate the motoring torque. Due to this electronic commutator BLDC motor can be more expensive when compared to corresponding brushed DC motor.

Other drawbacks of the brushless DC motor are the high speed and torque ripples and the increased current consumption, when the square wave current is switched from the one phase to another. However, the speed pulsation decreases with increasing rotor moment of inertia. A critical problem of this motor type is also the design of a permanent magnet rotor, because there is the possibility of the failure of magnet-rotor junction at high rotational speed and accelerations. As a result, the brushless DC motors are widely used for power outputs up to 20kW [6]. Above this power level vector-controlled induction motors are dominating. Therefore it can be concluded that the brushless DC motors can be used in low-cost belt-drives.

Permanent magnet synchronous machines (PMSM)

Permanent magnet synchronous machines emerged into servo drives since the second part of the 20th century and, nowadays, this motor type is widely spread in industry, especially in windmill generators and propulsion motors [8]. Main disadvantages of early permanent magnet motors were the risk of demagnetization of magnets by high stator currents during starting and the restricted maximum allowable temperature. The development of high-quality permanent magnet materials during the 1970s overcame these problems. PMSM's mechanical and electrical characteristics, especially the inductances, are highly dependent on the rotor structure. PMSMs can be realized either with embedded or surface magnets on the rotor. As the relative permeability of modern magnet materials is close to unity, the effective air gap becomes large with a surface magnet construction. As a result, the direct axis inductance of the machine remains low, which improves the overloading capability of the motor but at the cost of the reduced field weakening range. Another advantage of such a motor configuration is low inertia. Permanent magnet synchronous motors are very good alternatives for belt drives due to very good control characteristics and the absence of the mechanical commutator.

The drawback of PMSM is their relatively higher costs compared to the other types of motors.

Stepper motors

Stepper motors have become popular because they can be controlled directly by computers, microprocessors or programmable microcontrollers, thanks to their ability to rotate output shaft in angular steps corresponding to discrete signals fed into a controller.

The signals are converted into current pulses switched to the motor coils in fixed order and, thus, the motor works as an incremental actuator, which transforms digital pulses into analog output in form of shaft rotation. The rotational speed depends on the pulse rate and the incremental step angle, where the angle of rotation is dependent on the number of pulses received from the controller and the incremental step angle. These features make stepper motors appropriate to the open-loop position and speed control. Typical applications include disc head drives, small machine tool slides and printer head drives, where the motor might drive the head directly or via a belt. The following characteristics make the stepper motor suitable for servo drive applications:

- ✓ Stepper motors can work with a basic accuracy of ± 1 step in open-loop system. The inherent accuracy of the motor removes the requirements for the position and speed transducers and hence reduces the cost of the overall system.
- ✓ Stepper motors can generate high output torques at low angular velocities.
- ✓ Connection circuitry of the stepper motor is digital simplifying the interface to the programmable controller or control computer.
- ✓ Mechanical construction of the stepper motor is simple and robust.

However, an important point, which should be mentioned, is the phenomenon of resonance suffered by all stepper motors to some degree. As was mentioned above, stepper motor is controlled by pulses from the digital circuit. The step pulses are usually generated by an oscillator circuit controlled by an analog voltage, a digital controller or a microprocessor. A response to the sequence of five equally spaced step pulses in time is shown in Figure. 1.5.

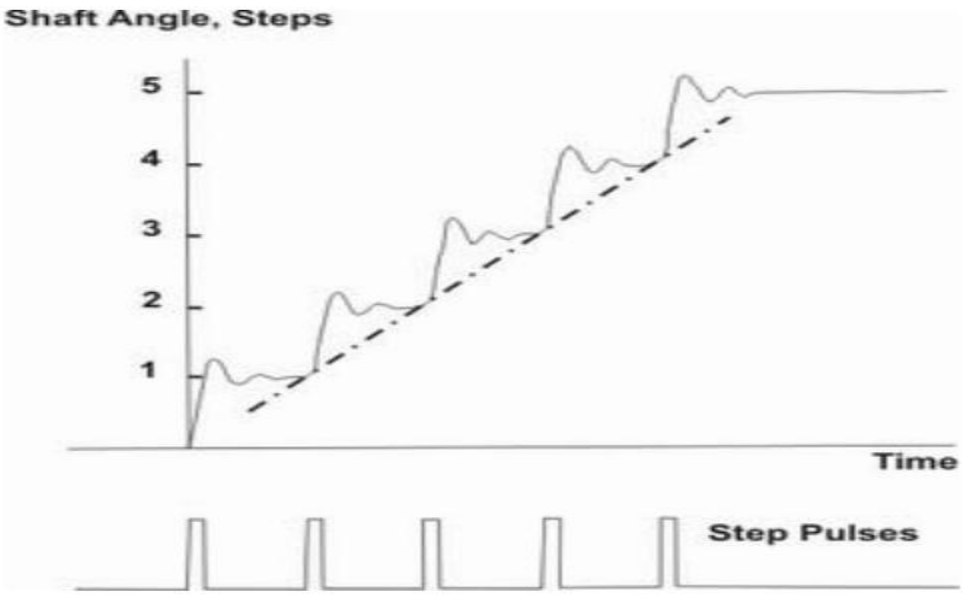

Figure 2.4 Typical step-response to low-frequency order of step pulses. [3]

Three main quantities can be noted from Figure.2.4. Firstly, the total shaft angle after five steps is generated by only the number of pulses, in such a way that the average speed of the shaft depends on the step pulse frequency. Hence, the higher frequency the less time is required for execution of the five steps. Secondly, a single step operation is not ideal, and therefore single-step times vary with motor size, step angle and the nature of load. Thirdly, it is necessary to

know the initial rotor position for the calculation of the absolute position after a step sequence, because the stepper motor is an incremental device. Normally, the step counter should be "zeroed" when the motor shaft is at its initial position.

As a consequence the stepper motor can be applied in very particular applications due to its specific characteristics.

Linear motors

Nowadays linear applications are more demanding than ever before. There are many brushless linear motors available for the motion control with large stroke length, high speed and accuracy, load capacity and stiffness at the moment. The linear motor concept is not new. Early machines had limitations in high speed operation due to commutation bar and brushes. Brushless servo motor technology and implementation electronics to drive them allow avoiding the above limitations. Commutation is manufactured electronically by Hall-effect sensors and therefore commutation is not limiting factor. Thus, brushless linear motors have a sum of advantages:

- ✓ High-speed operation. The maximum of linear motor speed is bounded only bus voltage and speed of control electronics. [11] Typical speed of linear motor is 3 meters per second with 1 micron resolution.
- ✓ High precision. The accuracy, resolution and repeatability of motor depend on controlled feedback device. Wide range of linear feedback devices allow to appropriate device limiting only control system bandwidth.
- ✓ Fast response. The response rate of a linear motor driven device can be over 100 that of a mechanical transmission.
- ✓ Zero backlash. No backlash due to absence of mechanical transmission components.
- ✓ Maintenance free operation. There is no wear due to absence of contacting parts in modern linear motors.

Side by side with all benefits, list of drawbacks such as high cost, sizing, heating exists.

The usage of linear motors can prevent the using of non-desirable belts in the systems and therefore can increase the accuracy of the system. But such decision can have the big cost and sizing problems.

2.3 Speed and position feedback devices in motion control

The precise control of speed, position or acceleration requires appropriate measuring systems for detection controlled variable. In this case measured quantities are rapidly changing therefore necessary to consider dynamic relationship between input and output of measurement system. In contrast, measured variable can be changed slowly in some kind of systems, hence the static performance should be considered. Before considering the various forms of sensor, it is necessary to mention significant characteristics such as resolution and accuracy.

The resolution of feedback device can be described as a number of measuring step per revolution of the motor shaft, for instance, resolution for incremental encoder is number of pulses per revolution. For analog feedback devices such as resolvers, resolution refers to associated resolver-to-digital converters.

The accuracy of sensor can be described as position deviation within one measuring step.

In encoder accuracy directly depends on the eccentricity of the graduation to the bearing, the elasticity of the encoder shaft and its coupling to the motor shaft, the graduation and the electronic signal processing. For analog feedback devices the accuracy is influenced by the winding distribution, eccentricity of the air gap, uniformity of the air-gap flux and elasticity of the resolver shaft and its coupling to the motor shaft.

Tachogenerators

The DC tachogenerator is electromagnetic transducer that converts mechanical rotation into DC output voltage commonly used as speed feedback device. The output voltage is directly proportional to the rotational speed. The basic fundamentals of tachogenerators are the same as DC motor, besides, significant features of its operation are following:

- ✓ Linearity of the output; that is output voltage proportional to the shaft speed with defined linearity.
- ✓ Smooth output; the output voltage should be free from ripple in range of frequency where drive is operating
- ✓ Independence output voltage of temperature; the output voltage for given speed should be constant with changing temperature.

Nevertheless, output characteristics of the tachogenerators are not ideal. The peak-to-peak value of output ripple-voltage component is reached 5-6%, with using special equipment is around 2-3%. [6] The temperature influence on characteristics is existed and quality of this parameter is closely related to the design principle and materials used in manufacture of the tachogenerators. Also linearity of output voltage can be affected by hysteresis losses in the armature core, output current drain, and armature reaction and saturation effect particularly in very-high speed applications. In that way, application of tachogenerators can be quite reasonable in motion control systems if speed transducer is required.

Encoders

While the velocity can be determined from position measurements, encoders are able to provide a separate output which is proportional to the velocity. Encoders are widely used as position transducers in robotics and machine tools. Generally they are divided into two types: absolute and incremental and each of these forms consists of three elements: optical receiver, a light source and code wheel. As receiver normally is used phototransistor or light sensitive diode and as light source can be light-emitting diode or filament bulb as shown in Fig.1.8. The difference between encoder types is in construction of the code wheel and how the output signal is recognized by external control system.

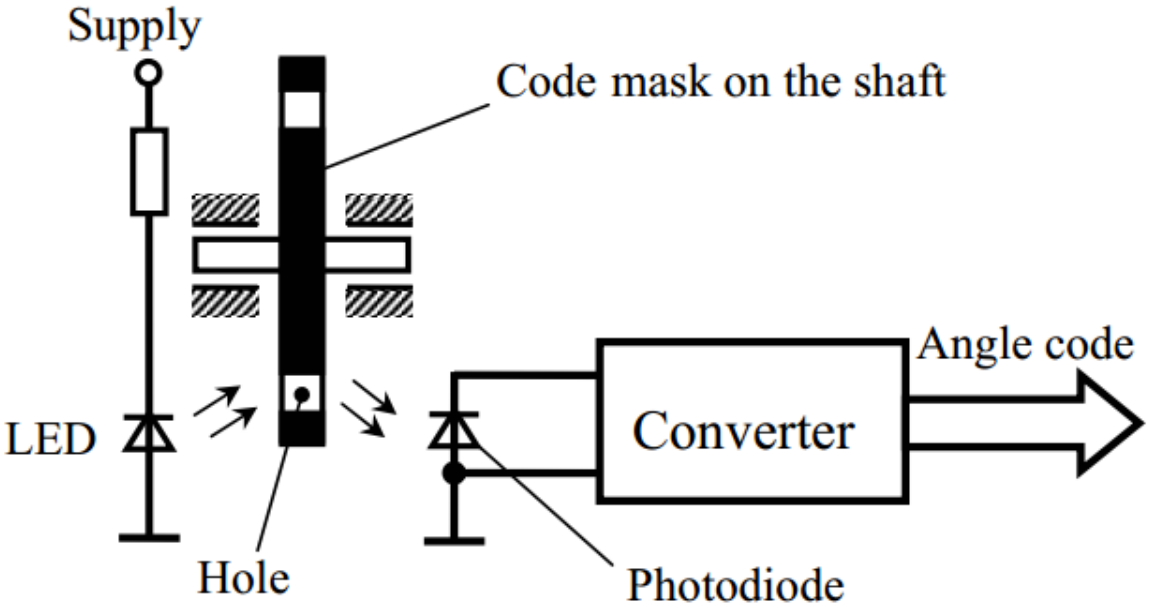

Figure.2.5. Photoelectric encoder [9]

Incremental encoders generate signal which increase or decrease measured value in incremental steps. On other hand, absolute encoder produces code values which directly correspond to the absolute position.

The significant advantage of the encoders is digital output in form of pulses train, and their frequency is not affected by temperature or weakening of long runs as in analog signal generator or resolver, therefore it is more reasonable using encoders in digital control systems.

Resolvers

The resolver is related to the synchro group. Synchro is meant the group of angular position sensing devices which can provide a rotational torque for light loads or signal which was caused by this rotational torque. A resolver is modified form of synchro which serves for resolving angular position into coordinate data for use in control system. It has two windings on the stator and one or two on the rotor and they are displaced by 90° to each other. The main purpose of the resolver is transformation Cartesian coordinate output signals from a polar coordinate input and ability to execute mechanical rotation of the resolver shaft. It is often to manufacture voltage

transformation ratio between primary and secondary windings to match into the next level of servo electronics. There are many types of resolvers existed in industry such as computing, brushless, multipole and so on. The properties that define this transducer type are high precision, low electrical errors and small sine deviation. [5] The basic configuration of the resolver is shown in Figure.2.6.

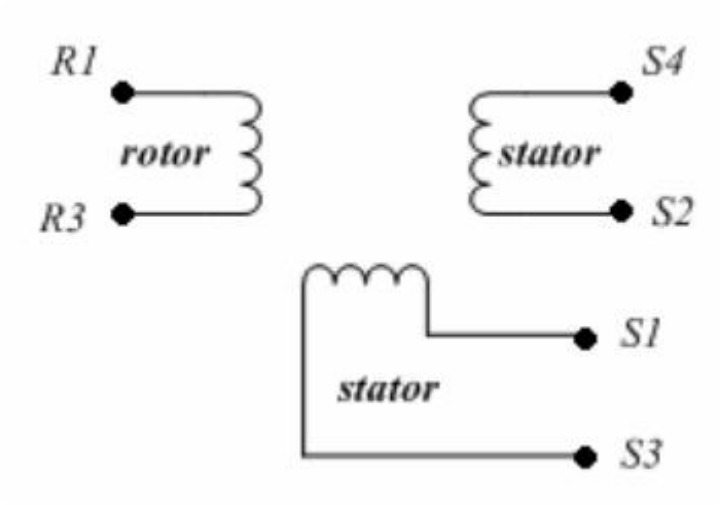

Figure 2.6 The basic configuration of resolver.

However, in practice error can be caused by order of factors: a difference between the primary/secondary transformation ratio, an electrical phase shift, or zero shift error between the two secondary windings. Besides, the output from the resolver is analog and for using in digital motion control systems resolver-to-digital converter is required. It is make a system more expensive and add limits on high-frequency operation. In addition, resolvers are very sensitive devices but limited by input signal range and has not compact dimensions, therefore using its in belt-drive systems is not reasonable.

Linear position sensors

There are many kinds linear position transducers presented in the industry. The systems considered above are widely spread in different application areas including belt drive systems; however, number of other position measurement systems are available are:

• Brushed potentiometers. The potentiometer principle can be applied in rotary and linear absolute-position transducers where output voltage depends of displacement.

It is possible to obtain good performance, in spite of non-uniform track resistance and brush contact. The typical servo devices based on brushed potentiometers have resolution of 0.05% of the full scale with accuracy of ± 0.1%. [6] The maximum operation speed is limited by the brushes.

• Linear variable differential transformers (LVDT). The operation of LVDC based on transformer with coupling between primary and secondary coils, is defined by the position of moveable ferromagnetic core. In such transducers the magnitude of the output signal is proportional to the displacement of the moveable core, and phase indicates the direction of the motion. In practice available travel length for LVDC changes from 1 to 600mm in a variety of linarites and sensitivities. There is no wear in mechanical components of LVDC because of absence of physical contact between the core and the coils. Due to small core size and mass, and lack of friction LVDC can be applied in high-response applications. In addition, this type of transducers can operate in hazardous environment with ambient pressures and temperatures due to rugged construction.

CHAPTER THREE

MODELING, DESIGN AND CONTROL OF THE OVERALL BELT DRIVE SYSTEM

3.1 Modeling of the electrical subsystem

The subsystems of the belt drive system: the electrical subsystem and the belt drive have been modeled in the next subsections. For a belt drive system consisting of two equal-radius pulleys, the torque applied to the driven pulley comes from the drive pulley.

The velocity of the driven pulley is reduced compared to that of the drive pulley. These conclusions infer that the external load added to the belt drive can be directly reflected to the electrical subsystem without changing the dynamics of the overall system except that the velocity of the driven pulley is a reduced version.

3.1.1 Modeling of the Permanent magnet synchronous motor

Modeling of the PM motor drive system is required for proper simulation of the system. A Three phase motor stator can be represented by an equivalent two phase representation with d and q corresponding to the direct and quadrature axis.

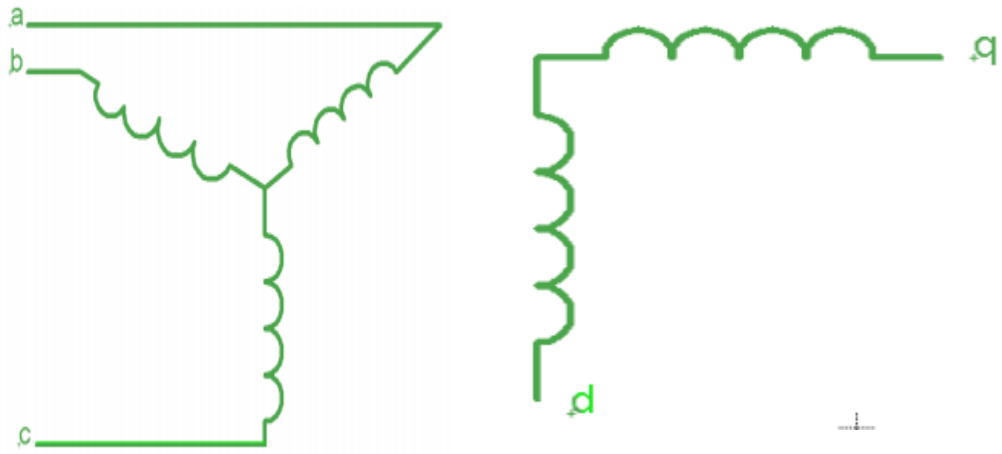

Fig.3.1. Three phase balanced stator windings and two –phase Equivalent

Hence the d and q model of the PMSM can be derived from the well-known model of the synchronous machine with the equations of the damper windings and field current dynamics removed.

Voltage equation

Here is the derivation of the electrical equations which are greatly simplified due to the concept of rotating transformation. The two axis voltage equations for the stator winding which are of an IPMSM (but is the same for SPMSM where L_d and L_q have the same value) are given by equations:

$$V_d = Ri_d + \frac{d\lambda d}{dt} - \omega_s \lambda_q \quad 3.1$$

$$V_q = Ri_q + \frac{d\lambda_q}{dt} + \omega_s \lambda_d \quad 3.2$$

Where: $\lambda_d = L_d i_d + \lambda_f$ 3.3

$$\lambda_q = L_q i_q \quad 3.4$$

Where i_d, i_q are stator currents; L_d and L_q are stator inductances; λ_d and λ_q are stator flux linkages in the d and q axes; & R is the stator resistance; λ_f is the flux linkage due to the rotor permanent magnet (PM) linking the stator

Substituting the equations (3.3) in (3.2) and (3.4) in (3.1) the dynamic equation gives a more convenient equation for equation below:

$$V_d = (R + L_d \frac{d}{dt}) i_d - \omega_s \lambda_q i_q \quad 3.5$$

$$V_q = \left(R + L_q \frac{d}{dt}\right) i_q + \omega_s \lambda_d i_d + \omega_s \lambda_f \quad 3.6$$

Equivalents circuits:

From the dynamic equations (3.5) and (3.6) the equivalent circuit of the PMSM can be derived for the stator q- axis and d- axis coordinates. During the steady state operation, the d- q axis currents are constant quantities. Hence the dynamic equivalent circuit can be reduced to the steady state circuit shown in figure (3.1).

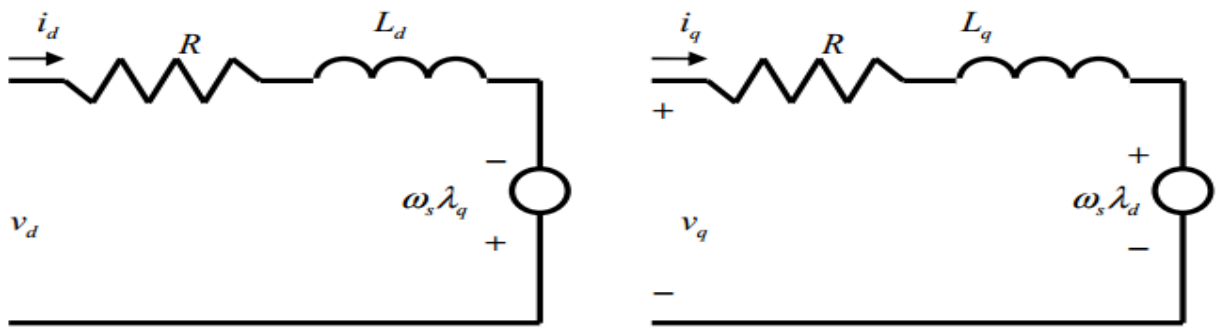

Figure 3.2 PMSM dynamic equivalent circuit of figure 3.1 from steady state equations

The electric torque generated on the PMSM is given by:

$$T_e = \frac{3}{2} P[\lambda_f i_q + (L_d - L_q) i_d i_q] \quad 3.7$$

Where, P denotes the number of the pole pairs of the PM on the rotor.

The mechanical dynamics of the PMSM drive system is given as:

$$T_e = T_l + \beta\omega_r + J\frac{d\omega_r}{dt} \quad 3.8$$

Where T_l- is load torque, β is damping coefficient $\omega_r$is the rotor angular velocity related to the inerter frequency by $\omega_r = \omega_s/P$, and J is the rotor moment of inertia.

Parks transformation and dynamic d-q modeling

The dynamic d-q modeling is used for the study of motor during transient and steady state. It is done by converting the three phase Voltages and currents to dqo variables by using parks transformation converting the phase Voltages variables $Vabc$ to $Vdqo$ variables is rotor reference frame the following equations are obtained:

$$\begin{bmatrix} V_q \\ V_d \\ V_o \end{bmatrix} = \frac{2}{3}\begin{bmatrix} \cos(\omega_s t) & \cos(\omega_s t - 120^o) & \cos(\omega_s t + 120^o) \\ \sin(\omega_s t) & \sin(\omega_s t - 120^o) & \sin(\omega_s t + 120^o) \\ 0.5 & 0.5 & 0.5 \end{bmatrix}\begin{bmatrix} V_a \\ V_b \\ V_c \end{bmatrix} \quad 3.9$$

Where; V_a, V_b and V_c are the phase Voltages in the stator windings and V_q, V_d are the Voltages in the d-q frame and V_o is the zero sequence component required to yield a unique transformation of the three phase stator quantities ; $\omega_s$is the inerter frequency.

Inversely the phase variables in abc frame can be resolved from the equation:

$$\begin{bmatrix} V_a \\ V_b \\ V_{oc} \end{bmatrix} = \begin{bmatrix} \cos(\omega_s t) & \sin(\omega_s t) & 1 \\ \cos(\omega_s t - 120^o) & \sin(\omega_s t - 120^o) & 1 \\ \cos(\omega_s t + 120^o) & \sin(\omega_s t + 120^o) & 1 \end{bmatrix} \begin{bmatrix} V_q \\ V_d \\ V_o \end{bmatrix} \qquad 3.10$$

The permanent magnets used in the PMSM are of high resistivity, the current induced in the rotor is negligible.

It is assumed that:

- ✓ There is no inductance leakage in the rotor
- ✓ The permeability of the magnetic material is considered unity
- ✓ The air gap inductances in the direct axis and the quadrature axis are the same
- ✓ The magnetic flux saturation is negligible
- ✓ The induced electromagnetic force (EMF) in sinusoidal.
- ✓ There are no field current dynamics

The mathematical model of PMSM can be summarized in state space representation as:

$$\begin{bmatrix} \frac{di_d}{dt} \\ \frac{di_q}{dt} \\ \frac{d\omega_r}{dt} \end{bmatrix} = \begin{bmatrix} -R/L_d & P\omega_r L_q/L_d & 0 \\ -P\omega_r L_d/L_q & -R/L_q & -P\lambda_f/L_q \\ -1.5P\lambda_f/J & 1.5P\lambda_f/J & -\beta/J \end{bmatrix} \begin{bmatrix} i_d \\ i_q \\ \omega_r \end{bmatrix} + \begin{bmatrix} V_d/L_d \\ V_q/L_q \\ -T_l/J \end{bmatrix} \qquad 3.11$$

The mathematical model of the PMSM is multivariable, nonlinear and strongly coupled system. Its speed and electromagnetic torque are difficult to be controlled by external signal. One of the effective control strategies is the vector control.

Vector control of PM motors

The vector control of the PM synchronous motor is derived from its dynamic model.

Consider a set of balanced three phase currents as input to the stator windings.

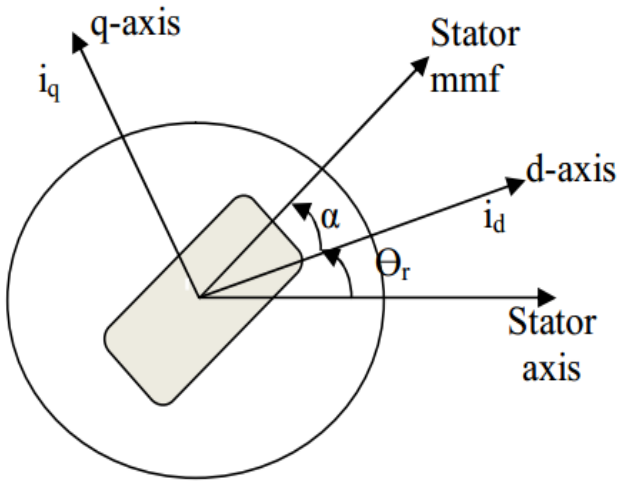

Figure 3.3 motor axis

Here:-

$$i_a = I_m \sin(\omega_r t + \alpha) \quad 3.12$$

$$i_b = I_m \sin(\omega_r t + \alpha - {}^{2\pi}/_{3}) \quad 3.13$$

$$i_c = I_m \sin(\omega_r t + \alpha + {}^{2\pi}/_{3}) \quad 3.14$$

Writing equations from (2.12) to (2.14) in the matrix form:

$$\begin{bmatrix} i_a \\ i_b \\ i_c \end{bmatrix} = \begin{bmatrix} \cos(\omega_r t + \alpha) \\ \cos(\omega_r t + \alpha - {}^{2\pi}/_{3}) \\ \cos(\omega_r t + \alpha + {}^{2\pi}/_{3}) \end{bmatrix} (I_m) \quad 3.15$$

where; α is the angle between the rotor field and stator current phasor, ω_r is the electrical rotor speed.

The currents obtained are the stator currents that must be transformed to the motor reference frame with the motor speed ω_r using Parks transformation. The d-q axis currents are constants and in rotor reference frame since α is a constant for a given load torque.

For this reason the q-axis current is called a torque producing component of the stator current and the d axis current is called the flux producing component of the stator current.

Now! Substituting the equation 3.15 in to 3.9 is obtained i_d and i_q in terms of I_m as follows:

$$\begin{bmatrix} i_q \\ i_d \end{bmatrix} = I_m \begin{bmatrix} sin\alpha \\ cos\alpha \end{bmatrix} \qquad 3.16$$

With the vector control, the state i_d can be governed by a current controller to satisfy the condition $i_d = 0$ so that the PMSM model is decoupled and simplified.

This is performed by making the toque producing i_q equal to the supply current I_m. This results in selecting the α angle to be 90 degrees according to equation 3.16. By making the i_d current equal to zero:

i.e. with the vector control, the current in the d-axis is governed :

$$i_d = 0 \qquad 3.17$$

The stator flux linkage in d-axis of equation (2.3) becomes:

$$\lambda_d = \lambda_f \qquad 3.18$$

The developed electromagnetic torque of equation (3.7) becomes:

$$T_e = \frac{3}{2} P\lambda_f \qquad 3.19$$

The resulting Mathematical model of the PMSM of Equation (3.12) is subsequently simplified to:

$$\frac{di_q}{dt} = \frac{-R}{L_q} i_q - \frac{-P\lambda_f}{L_q}\omega_r + \frac{V_q}{L_q} \qquad 3.20$$

$$\frac{d\omega_r}{dt} = \frac{1.5P\lambda_f}{J} i_q - \frac{\beta\omega_r}{J} - \frac{T_l}{J} \qquad 3.21$$

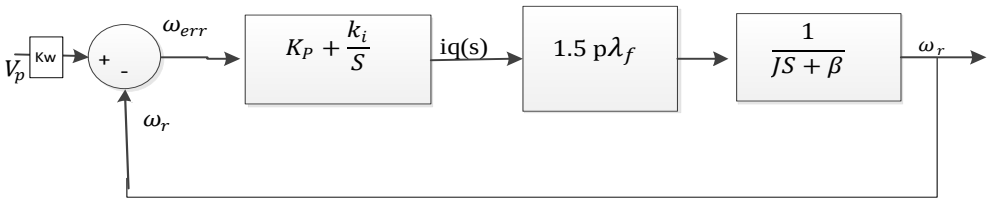

Figure 3.4.Equivalent schematic diagram of the PMSM Speed loop.

The model of the vector controlled PMSM can be obtained as:

$$\frac{\omega_r(s)}{V_p(s)} = \frac{1.5K_w \, P \, \lambda_f(K_p \, S + K_i)}{S^2 + \frac{(1.5PK_p\lambda_f + \beta)S}{J} + \frac{1.5P\lambda_f K_i}{J}} \qquad 3.22$$

3.2 Modeling of the belt drive system

Description of the system

The structure of the single axis belt drive is shown in Fig.3.5. This system consists of a servomotor, speed reducer and a belt drive. The belt drive is used for transformation of the rotational motion of the motor into a linear motion of the bagasse. The bagasse serves as load of the system.

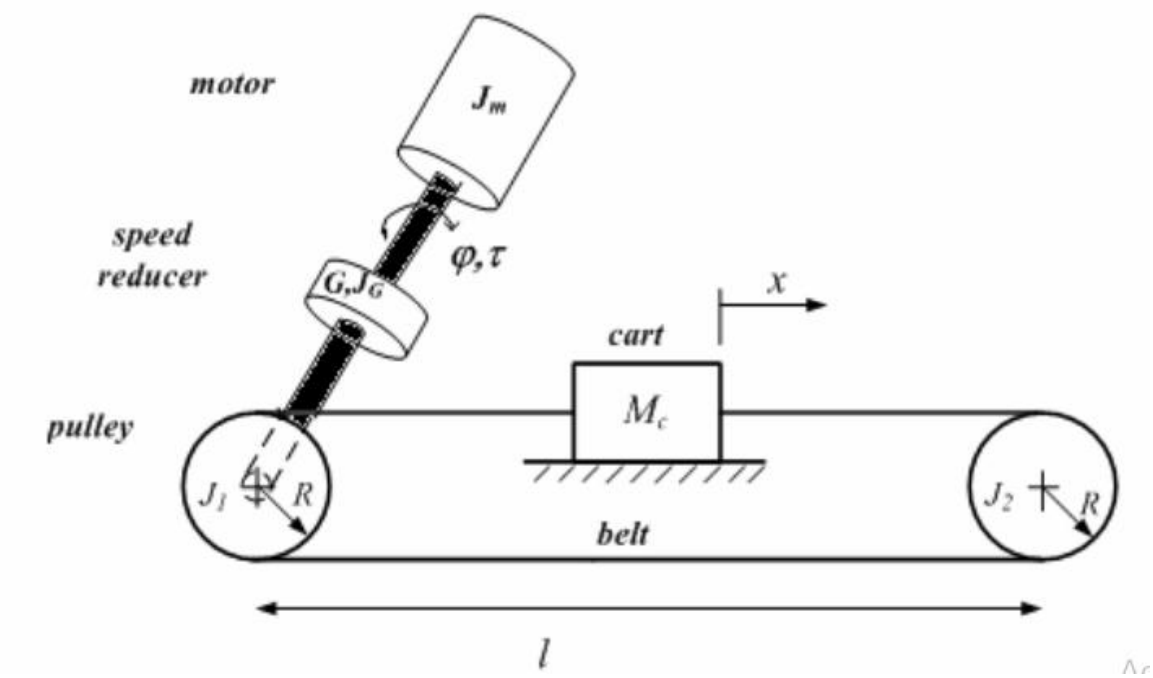

Figure 3.5 Linear belt drive system [12]

The belt drive system includes both driving pulley and driven pulley which stretch the belt irregularly. Such system represents non-linear distributed parameter model.

The following assumptions are supposed:

- The motor can provide a high-dynamic torque response with small time delay,
- Connection between motor shaft and driving pulley is rigid,
- The belt can be modeled by linear springs without mass,
- Friction is concentrated in the pulleys and the bagasse guidance and considered as external disturbances [11], for model design.

Thus, it was considered spring-mass model shown in Fig.3.6. The parameters and variables of the system are listed in Table 3.1.

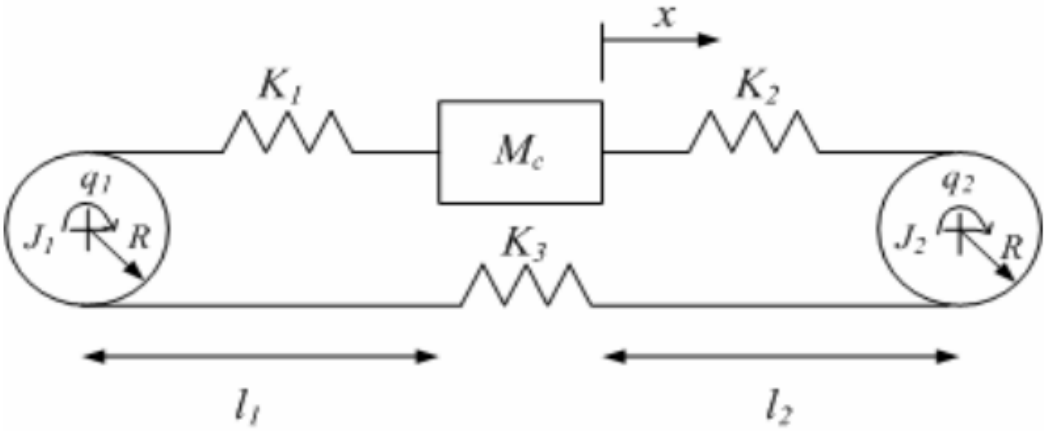

Fig.3.6 spring-mass model of the belt drive system [12].

Variables	Definitions
J_1,J_2	The inertia moments of driving and driven pulleys
J_m,J_G	The inertia moment of the servomotor and speed reducer
M_b	The bagasse mass
R	The radius of pulleys
K_1,K_2,K_3	The elasticity coefficients of the belt which change with respect to cart position
x	The bagasse position
τ	The torque developed by motor
q_1,q_2, φ r	The angular position of driving pulley, driven pulley and motor
G	The speed reducer ratio
l_1,l_2,l_3	The stroke length
τ_{f2} , τ_{f1} and f_f	The friction moments in the pulleys and friction force due to the load

Table 3.1 the parameters and variables of the belt drive system

Mathematical model for belt drive system, which is shown in Fig.3.6, is represented as equation system [11].

$$\left[J_1+G^2\left(J_m+J_G\right)\right]\ddot{q}_1+\tau f_1=G\tau-R\left[k_1(x)\left(Rq_1-X\right)-k_3\left(Rq_2-Rq_1\right)\right]$$

$$J_2\ddot{q}_2+\tau f_2=R\left[k_2(x)\left(X-Rq_2\right)-k_3(x)\left(Rq_2-Rq_1\right)\right] \qquad 3.23$$

$$M_b\ddot{x}+ff=k_1(x)\left(Rq_1-X\right)-k_2(x)\left(X-Rq_2\right)$$

Where $J_1+G^2\left(J_m+J_G\right)$ is the total moment of inertia, referred to the drive pulley and $G\tau$ torque, referred to the drive.

3.2.1. Elasticity of the belt

As was assumed, the belt has elasticity properties; therefore it is possible to change the length through the application external forces, caused by motor torque and bagasse mass. This quantity can be described by generalized Hooke's law in terms of the concepts of stress and strain. Stress is a quantity that is proportional to the force causing a deformation; strain is the measure of the degree of the deformation. In that way, according to generalized Hooke's law the tensile strain can be written as follows:

$$\varepsilon=\frac{\delta}{l_o} \qquad 3.24$$

where δ is the stretched part of the particle, when stretching with the force F, and $l_o$is the initial length of the particle. The value of the tensile strain is typically given by the manufacturer of the tooth belt axes.

An equation for the spring constants can then be derived from Hooke's law

$$F_{init}=K.x=K.\delta=K.\varepsilon.l_o$$

$$K=\frac{F_{init}}{\varepsilon}.\frac{1}{l_o} \qquad 3.25$$

where F_{init} is the initial tension of the belt and $l_o$is the initial length of the belt. With Eq. (3.25), functions for the position-dependent spring constants $K_1(x)$ and $K_2(x)$ can be found, and the value for the fixed spring constant K_3 can be calculated as:

$$K_1(x) = \frac{F_{init}}{\varepsilon}.\frac{1}{l1 + x}$$

$$K_2(x) = \frac{F_{init}}{\varepsilon}.\frac{1}{l2 - x} \qquad 2.26$$

$$K_3(x) = \frac{F_{init}}{\varepsilon}.\frac{1}{l3}$$

where l_1, l_2, and l_3 are the lengths of the belts and the x-axis spring constants K_1, K_2, K_3, are shown as a function of bagasse position.

3.2.2. Friction phenomena

Friction is present in all mechanical systems. Friction occurs when the surfaces of two pieces contact each other. Friction is widely studied especially in classical mechanical engineering.

The control engineer must understand the friction phenomena, especially if high-precision control is required. For example, the performance of the system may decrease and the steady-state error or limit cycles may occur because of friction. Friction can be divided into three different components: Coulomb friction, static friction (stiction), and viscous damping.

As can be seen, Coulomb friction, also called sliding friction, has a constant value, which changes only when the direction of the motion is changed. Stiction, also known as break-away friction, has a value other than zero only when the motor speed is zero, and elsewhere the value of stiction is zero.

The force required to overcome the static friction is called the break-away force. If the sliding friction is smaller than the static stiction, a Stribeck effect will occur. The viscous damping is changing as a function of motor speed.

Rolling friction is less significant than the sliding friction. Together, these forces make a system nonlinear.

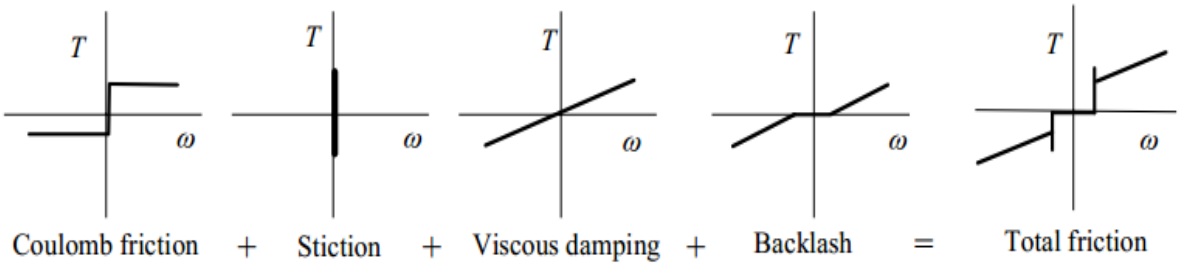

Figure 3.7.Total effect of friction phenomena in a system

Friction models

Modeling of different types of friction has always been a challenge for a controller designer, who would prefer that the frictions are linear and that only a viscous damping factor has to be modeled. However, in linear belt drives, the friction is non-linear, the Coulomb friction is high, and viscous damping is small, which makes it impossible to use only one viscous damping factor to illustrate the process friction and damping dynamics in the whole velocity range. A high value of a viscous damping factor describes the frictions with a reasonable accuracy at low speeds, but at high velocities, friction will be described as too large compared with a real system. Correspondingly, a low value of viscous damping describes frictions quite accurately at high speeds, but it does not provide satisfactory attenuation at a low frequency.

In the following, reviews of commonly used friction models are given.

Static friction: At zero velocity, static friction opposes to all motion until the applied force magnitude F_{app} is less than the maximum stiction force F_s.

$$F = \begin{cases} F_{app}, & if\ v = 0\ and\ |F_{app}| < F_s \\ F_s\ sgn(F_{app}), & if\ v = 0\ and\ |F_{app}| \geq F_s \end{cases} \qquad 3.27$$

where v is sliding velocity.

Coulomb friction: The friction force always opposes the relative motion. It is independent of the contact area and the relative velocity magnitude. In addition, Coulomb friction is proportional to the normal force and can be described by

$$F = F_c sgn(v) \qquad 3.28$$

where F_c is Coulomb friction.

Viscous friction: Viscous friction is proportional to the velocity and produced by the viscosity of lubricants. Mathematically viscous friction can be expressed as

$$Fv = K_v v \qquad 3.29$$

where k_v is the viscous friction coefficient.

Exponential model: A very common form of the combined friction model comprising of Coulomb and viscous frictions and also the Stribeck effect is

$$F(\dot{x}) = F_c sgn(\dot{x}) + (F_s - F_v)\exp\left(-(\dot{x}|\dot{x_s})^{\delta}\right) + F_v\dot{x} \qquad 3.30$$

where x_s and δ are empirical parameters.

Range of δ can be large [14]. The exponential model (3.30) gives a Gaussian model with δ=2, which is nearly equivalent to Lorentzian model. On the other side, δ=1 gives Tustin's model which given by:

$$F(\dot{x}) = F_c sgn(\dot{x}) + (F_s - F_v)\exp\left(-(\dot{x}|\dot{x_s})\right) + F_v\dot{x} \qquad 3.31$$

It is one of the best models to describe the friction force near zero speeds. Tustin was the first in feedback control who made a model with negative viscous friction (Stribeck effect). He predicts the oscillations at low speed. By variation parameters of exponential model can be obtained models for specific lubricants and conditions.

The Tustin's friction model was chosen for the design in the belt-drive system. It satisfactory describes the friction at low speeds and may help to model the possible oscillations in the beginning of the movement.

One drawback of this model is the discontinuity at zero speed, which causes the rate of change of the friction force to be infinite. To prevent this effect the sgn-function is replaced by saturation block with large slope coefficient.

3.3. System parameters

The total amount of mass being transported by the belt system is the summation of the mass bagasse and the mass of the belt itself.

$$M_t = M_{bagasse} + M_{belt} \quad 3.32$$

Applying the newton's second law M_t can be related to the force necessary to accelerate it.

$$F = M_t a \quad 3.33$$

where F is the effective belt tension and a is the linear acceleration of the belt.

In terms of angular measures the linear acceleration can be expressed as:

$$F = \frac{1}{2} D_1 M_t \alpha_1 = M_t \alpha_1 r_1 \quad 3.34$$

where $\alpha_1$is the angular acceleration of the driving pulley coupled to the motor shaft and r1 is the radius of the driving pulley. The force necessary to accelerate M_t is related to the torque about motor shaft as follows:

$\tau_{Mt} = \frac{1}{4} M_t D_1^2 \alpha_1 = M_t \alpha_1 r_1^2$ and

$$J_{Mt} = \frac{1}{4} M_t D_1^2 = M_t r_1^2 \quad 3.35$$

Moments of inertia of the driving and driven pulleys are supposed as equal and can be calculated from integral equation:-

$$J_1 = \int \rho\, r^2 dv$$

Where ρ is the mass per volume and can be defined as:

$$\rho = \lim \frac{\Delta m}{\Delta v} = \frac{dm}{dv}$$

$$dm = \rho dv$$

Thus moment of inertia of the pulley is described by expression:

$$J_1 = \int r^2\, dm = \frac{1}{2}\pi\rho l \int r^3 dm = \frac{1}{2}\pi\rho l r^4$$

where r is the radius of the pulley and l is the width of the pulley.

$$J_1 = \frac{1}{2}\pi\rho l r^4 = J_2$$

Now! $$J_{belt} = J_1 + J_2 + J_{Mt}$$

$$J_{belt} = \frac{1}{2}\pi\rho l r^4 + \frac{1}{2}\pi\rho l r^4 + M_t r_1^2$$

$$J_{belt} = \pi\rho l r^4 + M_t r_1^2 \text{ Where } r_1 = r_2 = r \qquad 3.36$$

Where J_1 is the moment of inertia of the driving pulley, J_2 is the moment of inertia of the driven pulley and J_{Mt} is the moment of inertia due to total amount of mass being transported.

The mechanical torque equation is given by:

$$\tau_m = \tau_l + \beta_{\omega m} + J\frac{d_{\omega m}}{d_t} \text{ Where } \omega_m = \omega_r * \frac{2}{P} \qquad 3.37$$

The electromagnetic torque:

$$\tau_e = \tau_l + \beta_{\omega r} + J\frac{d_{\omega r}}{d_t} \text{ Where } \omega_r = \omega_m * \frac{P}{2} \qquad 3.38$$

From the mechanical aspects belts are constant torque machines. That means constant level of torque is required to drive the belt regardless of the operating speed.
The mechanical part of the motor equation is derived using newton's second law which states the inertial load times the derivative of angular rate equals the sum of all torques about the motor shaft. By energy conservation the resultant torque on motor shaft must be equal to zero.

$$\tau_e - \tau_l - \tau_\omega - \tau_{\omega'} \qquad 3.39$$

Where τ_e is the electromagnetic torque, τ_ω is the torque associated with velocity of rotor, $\tau_{\omega'}$ is the torque due to rotational acceleration of the rotor and τ_l the load torque of the belt system

The electromagnetic torque is given by:

$$T_e = \frac{3}{2}(P)(\lambda_d i_q - \lambda_q i_d] \text{ But } i_d = 0$$

$$T_e = \frac{3}{2} P\lambda_d\, i_q$$

$$T_e = k_m\, i_q$$

$\tau_{\omega'}$ is written as:

$$\tau_{\omega'} = J\frac{d_{\omega r}}{d_t} \text{ where } J \text{ is the inertia of the rotor.}$$

The torque produced as the resultant of the rotor velocity is written as

$$\tau_{\omega} = \beta_{\omega r} \text{ where } \beta \text{ is the damping coefficient.}$$

Substituting the above equations:

$$k_m\, i_q - J\frac{d_{\omega r}}{d_t} - \beta_{\omega r} - T_l = 0 \qquad 3.40$$

Design of belt load torque

Consider the motion of the belt which creates friction between pulleys and the belt itself.

$$F_f = \mu N \qquad 3.41$$

Where μ the coefficient of friction between the belt and platform and N is the normal force acting to press the belt against platform. To relate the friction force F_f to the torque requirement for motor of the belt system, F_f can be related to the torque acting about the motor shaft as written below:

$$\tau_f = \frac{1}{2}F_f D_1 = F_f r_1$$

$$= \mu N r$$

$$\tau_f = \mu M_t g r \qquad 3.42$$

Recall that newton's second law for angular motion relating torque, mass inertia and acceleration is given by:

$$\tau = J\alpha$$

And for the belt drive system:

$$\tau = J_{belt}\alpha_1 \qquad 3.43$$

Therefore, the total torque produced by the belt system is written as follows by combining the equation 3.42 and 3.43

$$\tau_{belt} = (J_1 + J_2 + J_{mt})\alpha_1 + \tau_f$$

$$\tau_{belt} = J_1\alpha_1 + J_2\alpha_1 + J_{mt}\alpha_1 + \mu M_t g r \qquad 3.44$$

Since the belt drive system has a constant velocity

$$\tau_f = \mu M_t g r \text{ Which is load the torque} \qquad 3.45$$

3.4. Design of PI controller

In process control today, more than 95% of the control loops are of PID type, most loops are actually PI control. In the control of dynamic systems, no controller has enjoyed both the success and the failure of the PID control. There is actually a great variety of types and design methods for the PID controller. The most used type of PID controller is PI controller. What is a PI controller? The acronym PI stands for Proportional-Integral control. Each of these, P, and I are terms in a control algorithm, and each has a special purpose. In the field of electrical drives PI regulators are employed for motor control. The variables to be controlled are position, speed, torque, and current or voltage. The fact that the measurement of these signals can contain considerable noise (high frequency) makes the PI structure without the derivative part more suitable. And in fact PI controller is enough for first order systems.

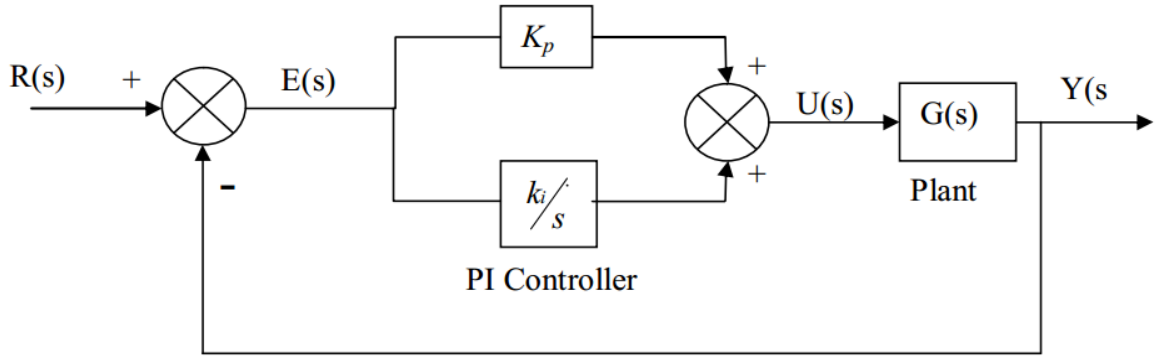

Figure 3.8: PI control System

3.4.1 Speed control of PMSM

Speed Control Systems allow one to easily set and adjust the speed of a motor. The control system consists of a speed feedback system, a motor, an inverter, a controller and a speed setting device. A properly designed feedback controller makes the system insensible to disturbance and changes of the parameters.

The purpose of a motor speed controller is to take a signal representing the demanded speed, and to drive a motor at that speed. Closed loop speed control systems have fast and dynamic response, but become expensive due to the need of feedback components such as speed sensors.

Speed controller calculates the difference between the reference speed and the actual speed producing an error, which is fed to the PI controller. PI controllers are used widely for motion

control systems. They consist of a proportional gain that produces an output proportional to the input error and an integration to make the steady state error zero for a step change in the input. The equivalent schematic diagram of the speed loop is determined from Equations (3.8), (3.20) and (3.21) as shown in Figure 2.5, where V_p is the input voltage signal,K_ω is the gain constant, $K_p$and K_i are the proportional and the integral gains, respectively.

$$J\frac{d}{dt}\omega_r = 1.5\ \mathrm{p}\lambda_f i_{qs} - \beta\omega r - T_l \qquad 3.46$$

Take the Laplace transform by neglecting T_l

$$JS\omega_r(s) = 1.5\ \mathrm{p}\lambda_f i_{qs}(\mathrm{s}) - \beta\omega_r(s)$$

$$(JS+\beta)\omega_r(s) = 1.5\ \mathrm{p}\lambda_f i_{qs}$$

$$\frac{\omega_r(s)}{i_{qs}(\mathrm{s})} = \frac{1.5\ \mathrm{p}\ \lambda_f}{JS+\beta} \qquad 3.47$$

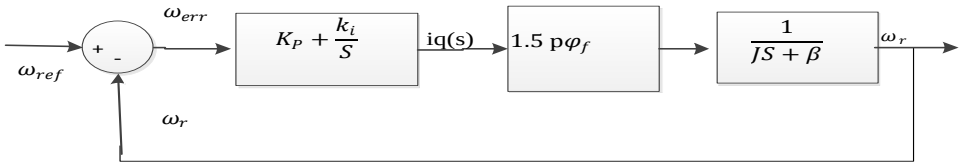

Figure 3.9: Block diagram of PMSM speed controller

Here the model of vector controlled PMSM can be obtained as follows:

$$\frac{\omega_{ref}(s)}{\omega_r(\mathrm{s})} = \frac{1.5\ \mathrm{P}\ \lambda_f(K_p\ S + K_i)}{S^2 + \frac{(1.5P\lambda_f K_p+\beta)S}{J} + \frac{1.5P\lambda_f K_i}{J}} \qquad 3.48$$

$$\frac{\omega_n^2}{S^2+2\zeta\omega_n S+\omega_n^2} \qquad 3.49$$

Comparing the second order closed loop system performance in equation (3.49) with equation (3.48), the values of kp and ki in terms of motor parameters in in appendix 2 are found in equation (3.50) and equation 3.51.

$$K_i = \frac{2}{3}\left(\frac{J\omega_n^2}{P\lambda_f}\right) \qquad 3.50$$

$$K_p = \frac{4}{3}\left(\frac{J\omega_n\zeta-\beta}{P\lambda_f}\right) \qquad 3.51$$

CHAPTER FOUR

SIMULATION AND DISCUSSION

This chapter of the thesis is concerned with the simulation results of the closed loop control of the system using PI with Matlab/Simulink. The proposed control system is represented by Figure1.1 is designed for simulation by Matlab/Simulink model. Simulation results are presented and discussed to show the effectiveness of the proposed drive system based on speed and position tracking of the belt driving system at different operating conditions. For studying the performances of proposed system, a series of simulations and measurements have been carried out. In this respect, the dynamic response of the proposed speed tracking control algorithm is studied under different speed command.

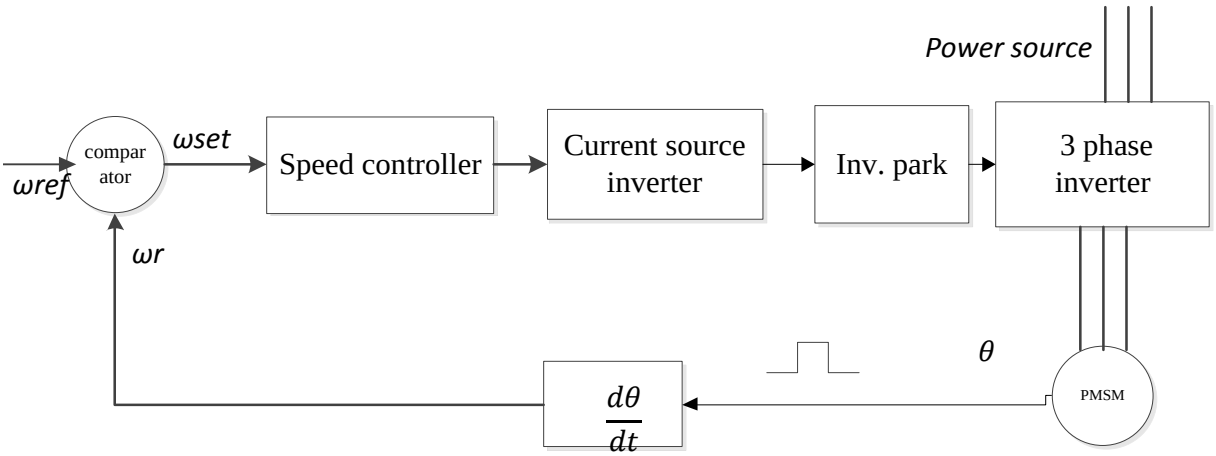

Figure 4.1.general block diagram of the PMSM drive system

4.1 Simulink model of PMSM Drive system

The overall Matlab/Simulink model of the PMSM drive and Control system is shown in figure 4.2. All the components of the real drive system are modeled to study the simulation result.

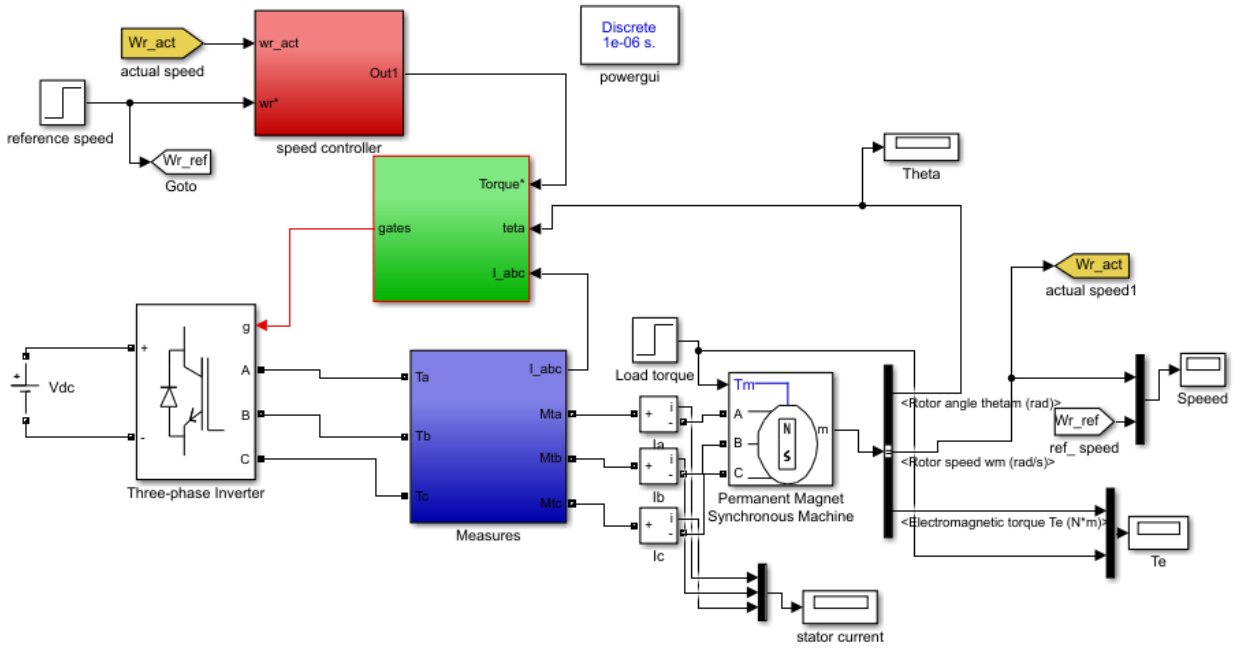

Figure 4.2: Matlab/Simulink Model of the PMSM drive.

The overall Matlab/Simulink model of the PMSM drive allows simulating the behavior of the machine using PI algorithm for different operating modes.

4.1.1 Discussion for Simulation results of PMSM Drive system

The simulation result of the belt drive system was carried out to assess its performance. Knowledge of motor's parameter is important for this simulation since the system nonlinearities are highly parameter dependent and the effect of the parameter variation was tested based on different condition that are put on their effects on robustness of the speed tracking control.

The first simulation result for the belt drive system is the three phase stator current which is generated by the three phase current source inverter. This three phase current source inverter is controlled for appropriate stator current generation. These three phases current should be equal magnitude and 120° phase shift with each other for appropriate rotating flux generation as shown in Figure 4.3.

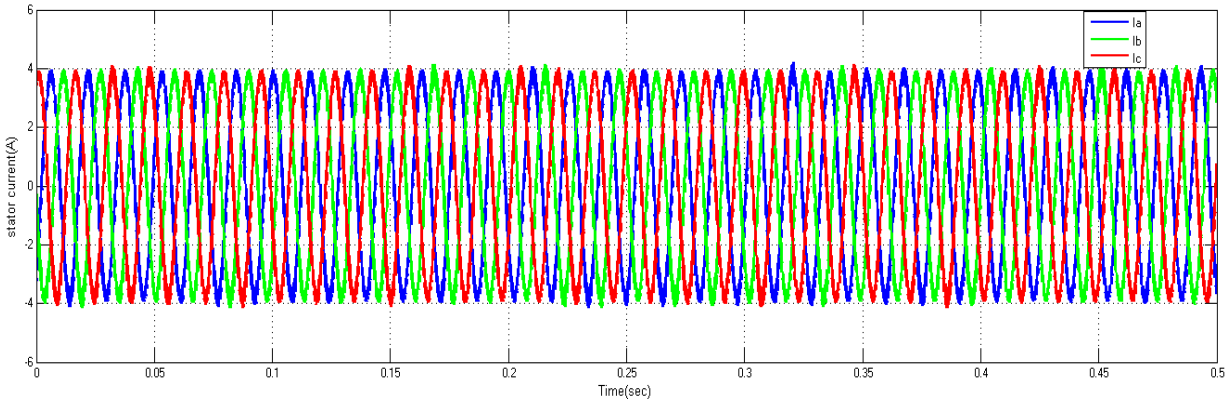

Figure 4.3 three phase stator current

As it has been seen from the Figure 4.3, the appropriate stator phase current is generated with good accuracy. Hence the system can feed the appropriate stator voltage to the motor. If the voltage applied to the motor is applied with appropriate magnitude and frequency, the speed of the motor is respected as set to the reference value. The simulation result of the proposed belt drive system is discussed in terms of:

- ✓ Set point tracking capability.
- ✓ Torque response quickness.

Set point tracking capability

First, response of the system is tested for step speed input and the speed response for consecutive step levels is tested. It shows the convergence of the actual rotor speed to the reference speed.

As shown in Figure 4.4 proposed system tracks both the step and square signals reference input. This shows the tracking performance of the actual speed to the reference speed can be examined by changing the reference of the system with the maximum steady state error of 0.0027% and good transient performance with rise time less than 0.1 second.

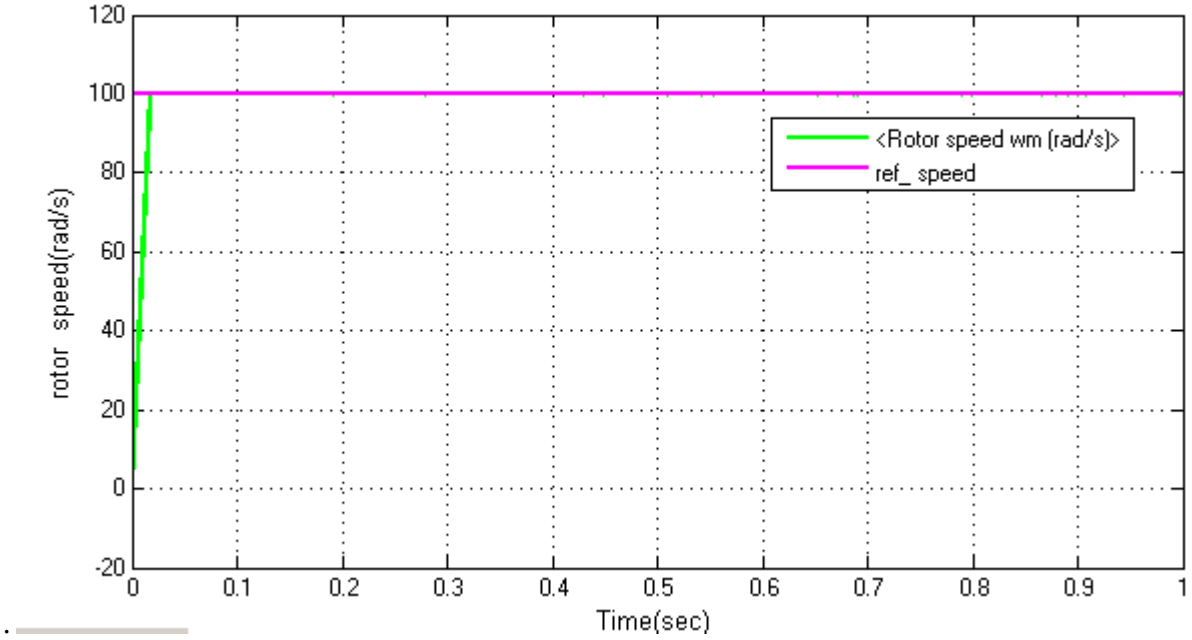

Figure 4.4: Speed response of the machine for 100rad/sec reference speed.

- ✓ **Torque response quickness.**

To show the impact of torque response quickness on the speed and position tracking control of PMSM belt drive system, speed response for torque variation is simulated based on full load and no load torque conditions.

4.1.2 Speed response under no load condition

Figure 4.5 shows the developed electromagnetic torque when the drive system is running under no load torque condition. The starting torque until 0.03sec is around 5Nm which is due to primarily the acceleration of the rotor to reach to the steady speed of 100 rad/sec. The starting torque is higher when compare to the steady state value. So this generated torque is meant to support acceleration of the rotor and the friction retard without the load torque (TL=0). However, after 0.03sec the generated torque is reduced almost to 0Nm to support only the approximately zero retard friction.

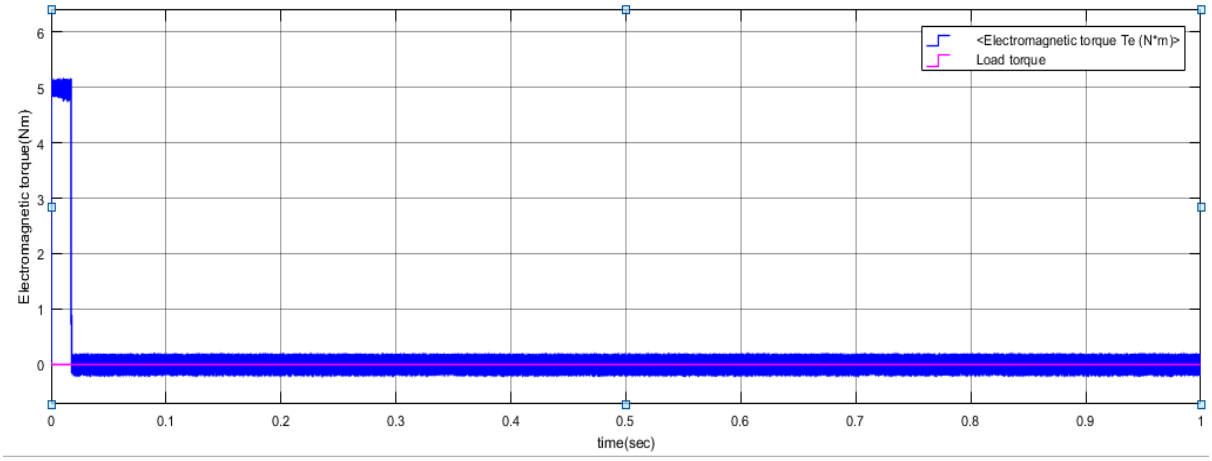

Figure 4.5: Developed electromagnetic torque under no load torque condition.

It is clear that the current is non-sinusoidal at the starting and becomes sinusoidal when the motor reaches the controller command speed at steady state. Figure 4.6 shows the three phase currents (ia , ib and ic) drawn by the motor when the motor is operating at a reference speed.

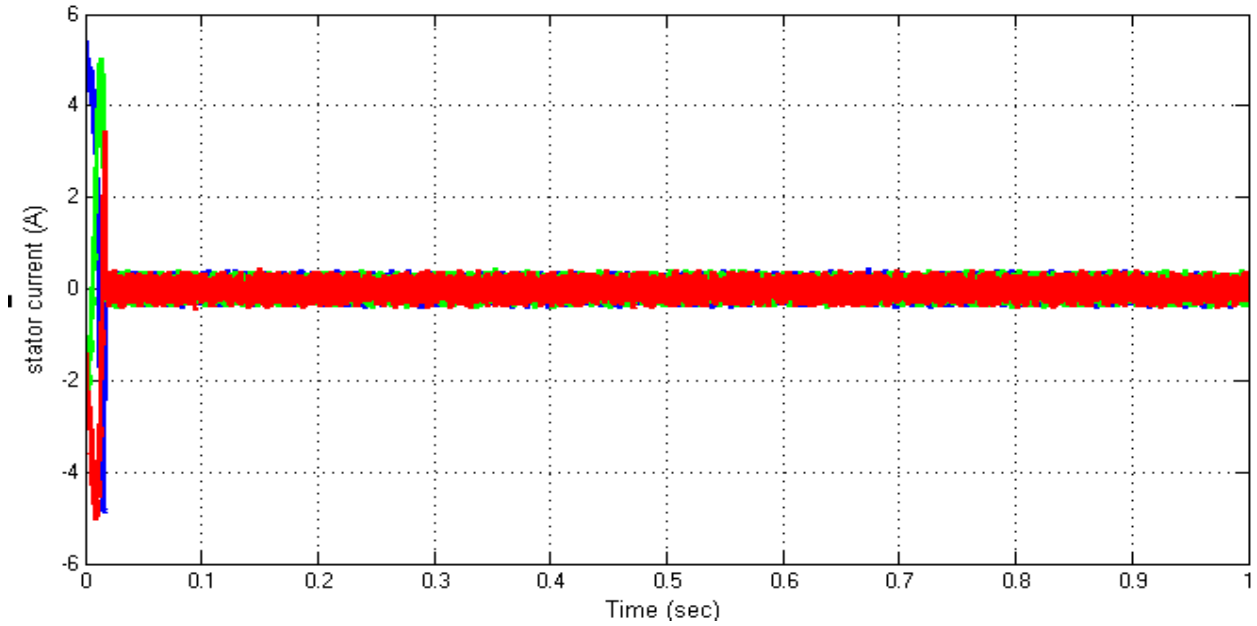

Figure 4.6: i a, ib &ic Currents as motor accelerating to 100 rad/sec speed input.

Figure 4.6 shows the speed response of the machine for two ramped step speed level desires.

First the speed desire is set to be 100rad/sec. Then the speed changes instantly at t = 0.5s and attains it steady speed of 160 rad/sec.

Figure 4.7 shows the speed response for two step input speed level commands and Figure 4.8 shows the current drawn by the machine for the two ramped step speed level command.

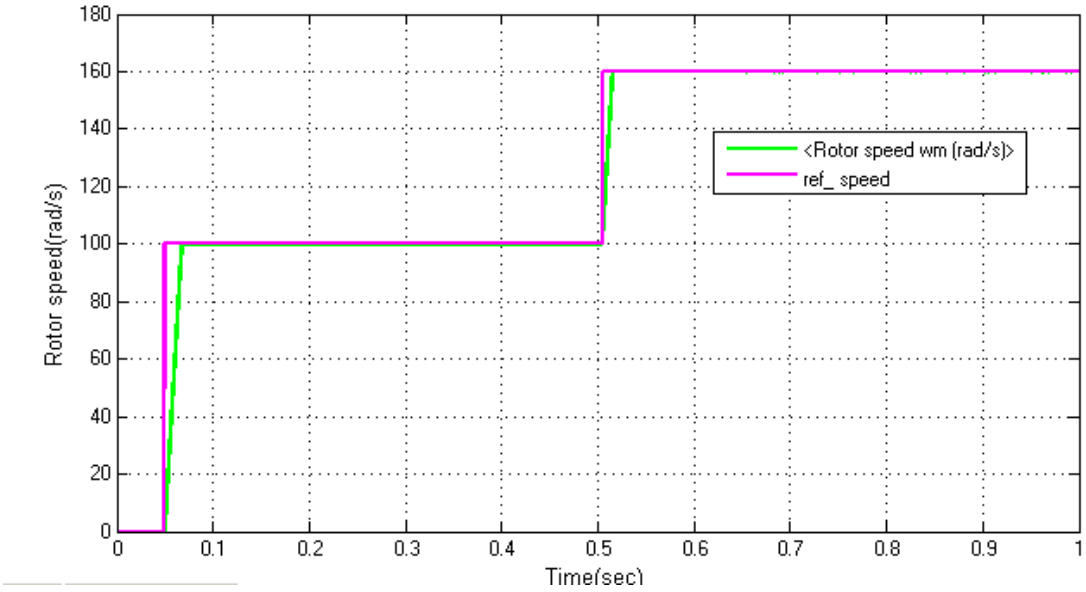

Figure 4.7: Reference speed and speed response at two ramped step speed levels.

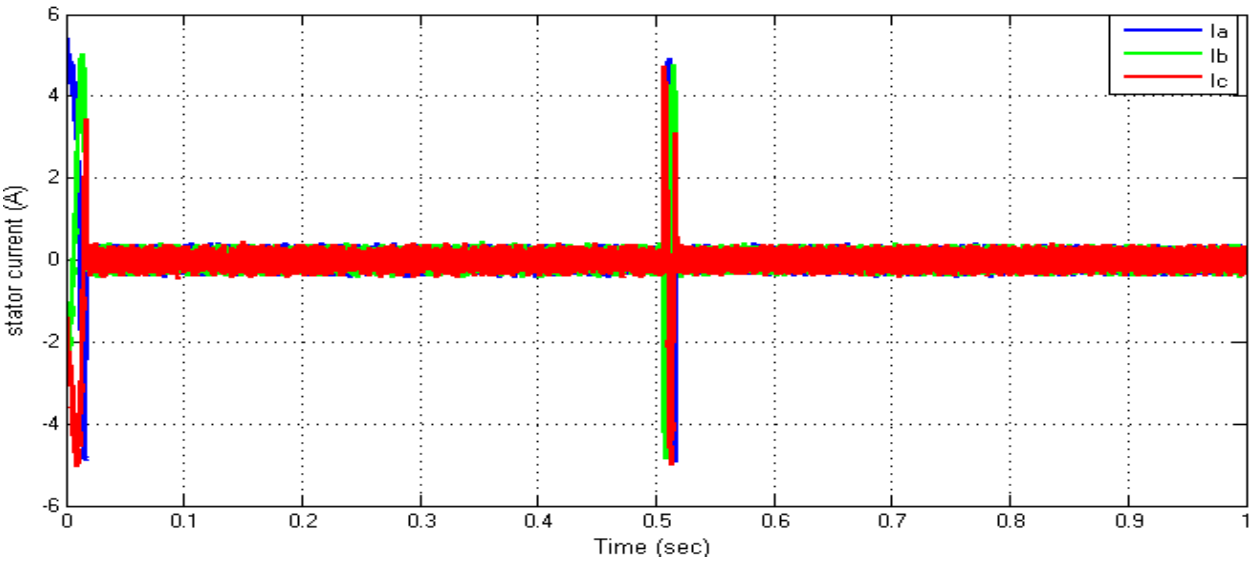

Figure 4.8: Current drawn by the motor for two level speed commands.

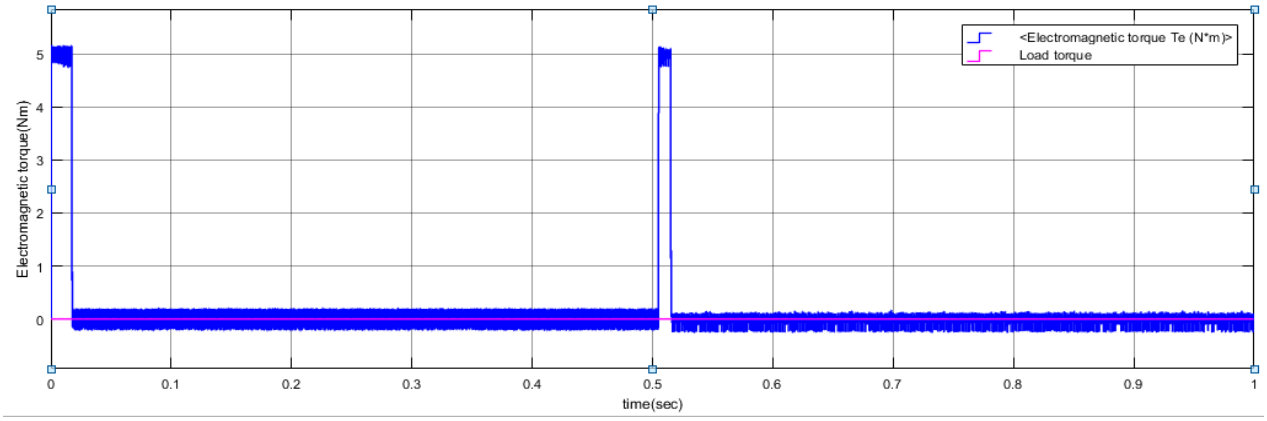

Figure 4.9: Electromagnetic torque generated for the two step level speed input.

4.1.3 Speed response of PMSM Drive system with a load torque

To find the torque response quickness the PMSM belt driving system is stared with 0Nm load torque and this value is increased to 4.05Nm after 0.05 second this result a drop in motor speed. This happens because of the mismatch in the torques, i.e. the developed torque is less than the load torque. To compensate for this mismatch, the controller increases the developed torque then the motor speed increases and comes back to the set point as shown in Figure 4.9. From the this result the steady state error is zero and the settling time is less than 0.05 second, this shows that the drive system is good tracking performance under full load condition.

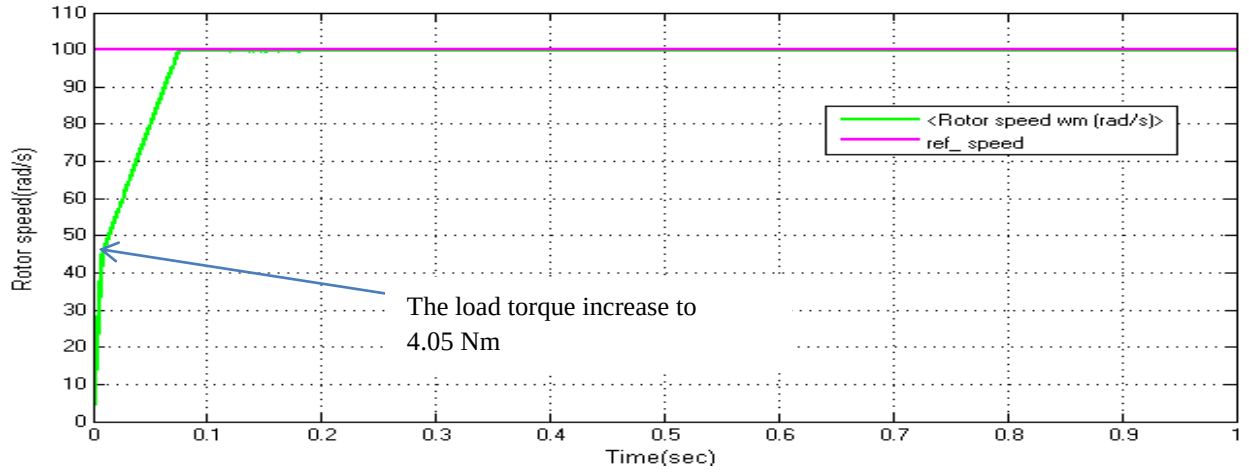

Figure 4.10: shows the speed response of the motor with load when the motor is commanded at a reference speed of 100rad/sec

Figure 4.11 shows the load torque track the developed electromagnetic torque with good steady state and transient response. The developed electromagnetic torque was 5.0Nm until 0.05 sec which is due to primarily the acceleration of the rotor to reach to the steady speed of 100 rad/sec. So this generated torque is meant to support acceleration of the rotor and the friction retard with the load torque (TL=4.05Nm). However, after 0.05sec the generated torque is reduced almost to 4.05Nm.

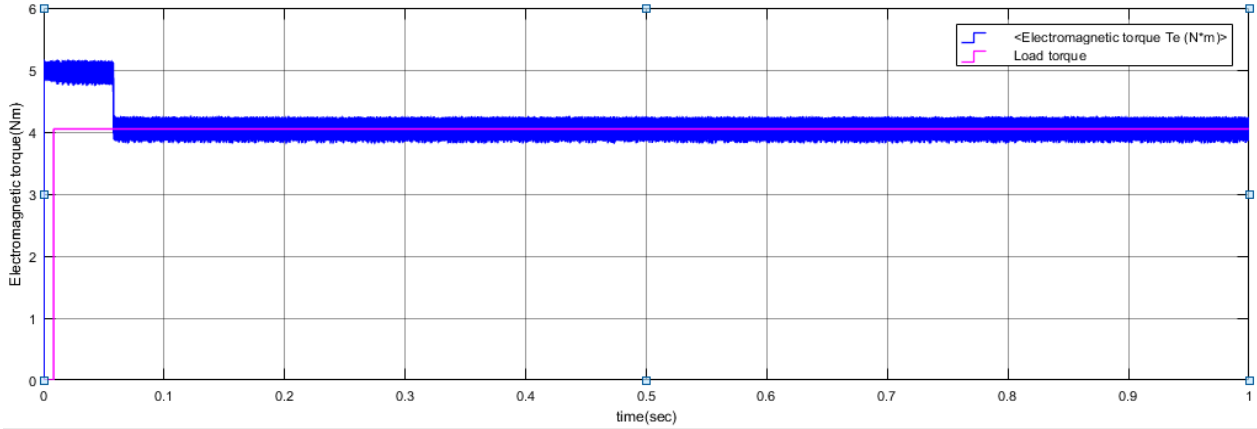

Figure 4.11 the developed electromagnetic torque with load torque 4.05Nm

Figure 4.12 shows the three phase currents (ia, ib and ic) drawn by the motor when the motor is operating at a reference speed and load torque 4.05Nm. From this result the three phase stator current is equal magnitude and 120° phase shift with each other for appropriate rotating flux generation.

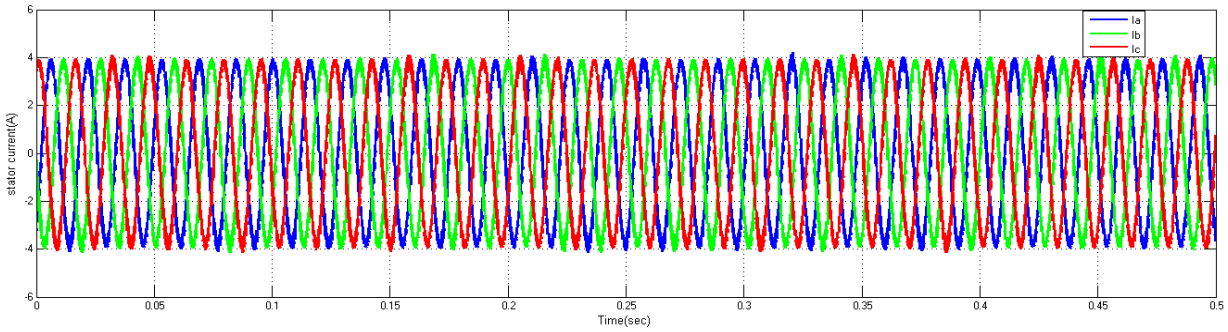

Figure 4.12 the three phase currents (ia, ib and ic) with load torque 4.05N

4.2 Simulink model of the belt drive system

A Simulink model of the belt drive system was developed using components from the MATLAB Simulink library. This is a particularly useful add-on to Simulink that provides models for a wide range of power electronics devices and control structures. The belt drive system structure was simulated using the theory outlined in Chapter 3 of this thesis and is shown in Figure 4.13.

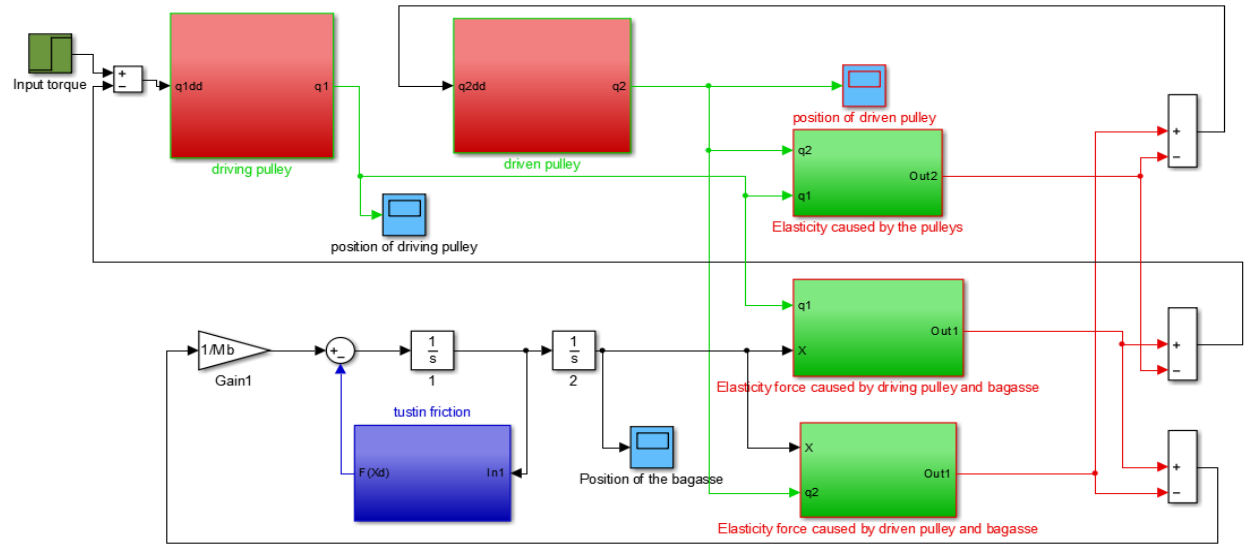

Figure 4.13 Simulink model of belt-drive system.

The ramp response for the accurate position control of driving pulleys, driven pulley and the position of the bagasse is represented in Figure.4.14, Figure4.15 and Figure 4.16 respectively. It can be seen that the ramp response satisfies the control requirements.

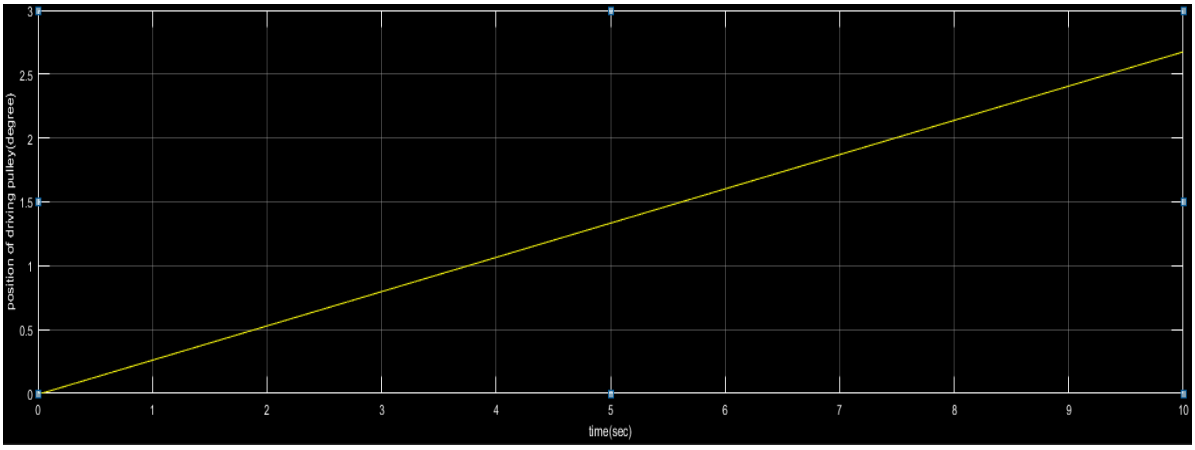

Figure 4.14 Position of the driving pulley

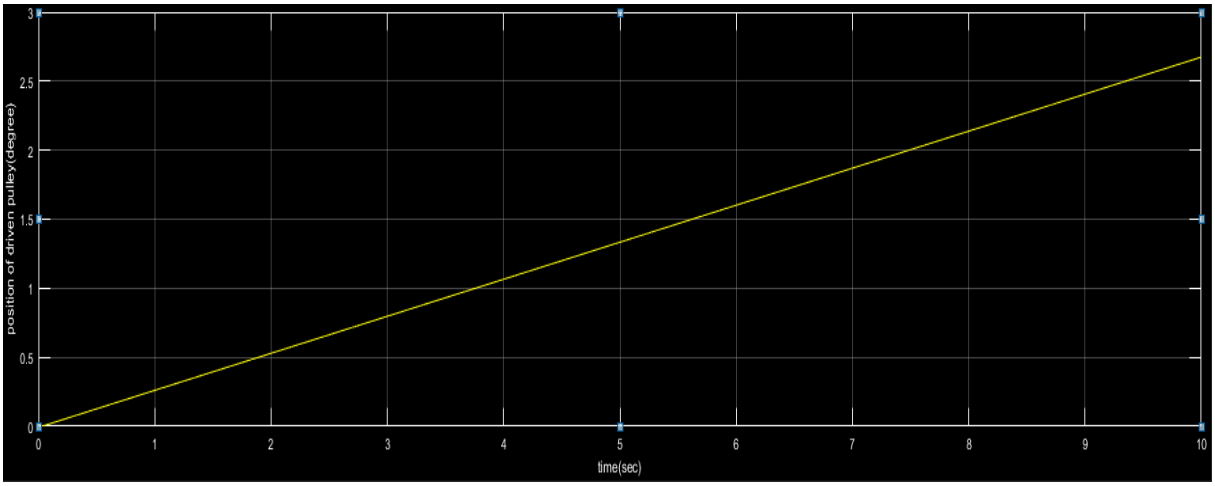

Figure 4.15 Position of the driven pulley

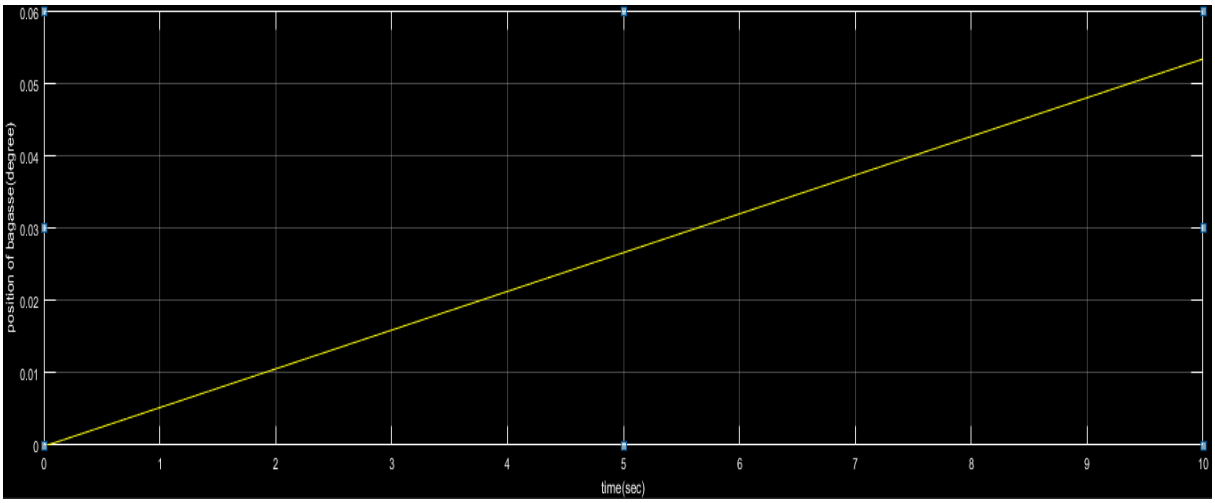

Figure 4.16 Position of the bagasse

The effective position control for a linear belt drive system based on the PI controller based model was designed. A dynamic model and feedback controller were developed for the system taking into account the nonlinearities with friction model and the belt elasticity. Permanent magnet synchronous motor produces shaft rotation coupled with the driving pulley and moves the bagasse in good position accuracy.

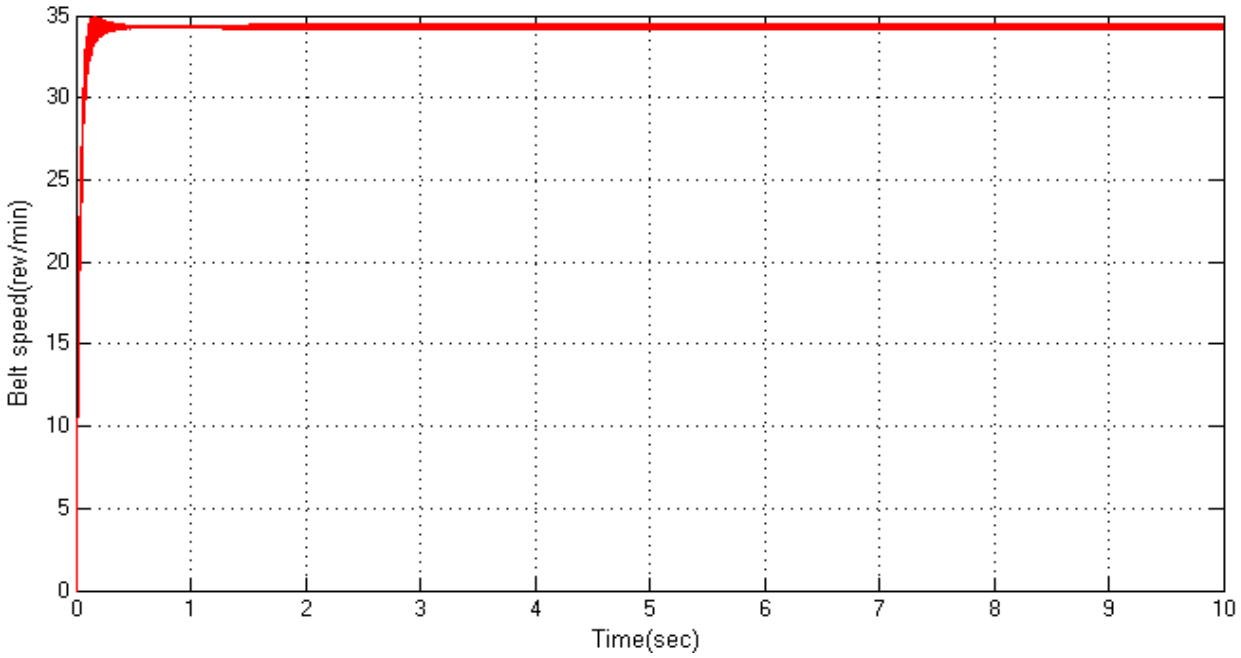

Figure 4.17 Speed of the belt drive system

The step response for the accurate speed control of belt drive system is represented in Fig.4.17. It can be seen that the step response satisfies the control requirements: overshoot is 0.006% and the settling time 0.0015sec. Hence it was concluded that the simulation model is adequate for the given belt-drive system.

CHAPTER FIVE

CONCLUSION

As result of the work a modeling and design of the belt drive system and its PI control was developed. The designed model describes the system behavior with adequate accuracy. Friction and belt elasticity phenomena impact was taken into account in the developed model. The PI control based on the speed feedback was developed. This control was applied to the designed dynamic model to show its effectiveness by simulations. Using the developed model the Simulink model of the controller with the help of MATLAB instruments can be performed.

The developed speed control system ensures allowable error value. Also the damping and the operating speed of the closed loop system are satisfactory with overshoot is 0.006% and the settling time 0.0015sec. As a conclusion, the specified position and speed control requirements were attained and high accuracy of the belt drive system is achieved with the help of PI controller. The position and speed error is effectively eliminated.

References:

[1] Hungles, A., 2003. Electric motors and drives: Fundamentals, types and applications. Printed by Newnes, Manchester. ISBN 0-7506-1741-1

[2] Younkin, G., 2003. Industrial servo control systems: Fundamentals and applications.

[3] Kerrkanen K., 2006.Dynamic analysis of belt-drives using the absolute nodal coordinat formulation. /PhD work Lappeenranta University of Technology. ISBN 952214-193-3

[7] Toshihiro, S., Tsuneo, K., 2004. Motor drive technology: History and visions for the future. 35th Annual IEEE Power Electronics Specialists Conference, p.2-9.

[5] Drury, B., 2001. The Control Techniques Drives and Controls Handbook, Published by the Institution of Electrical Engineers, London. ISBN 0-85296-793-4

[6] Crowder R. M., 1995. Electric drives and their controls, Clarendon Press, Oxford. ISBN 0-19-859371-6

[7] Mikerov A.G., Djankhotov V.V., 2002. Small electrical machines and drives. SaintPetersburg Electrotechnical University “LETI”, Russia

[8] Puranen, J., Induction motor versus permanent magnet synchronous motor in motion control applications: a comparative study. / PhD work Lappeenranta University of Technology. ISBN 952-214-296-4

[9] Barret J., Harned T., Monnich J. Linear motor basics. Parker Hannifin Corporation.

[10] Pyrhonen J., 2006. Electrical Drives 2006/2007, Lecture notes, LUT, Finland.79

[11] Hace, A., Jezernik, K., Sabanovic, A., SMC with disturbance observer for a linear belt-drive, IEEE ISIE 2005, June 20-23, Dubrovnik, Croatia.

[12] Serway R.A., 1982.Physics: For scientists and engineers. ISBN 0-03-057903-1

[13] Ge S.S., Lee T.H., Ren S.X., 1999.Adaptive Friction Compensation of Servo Mechanisms, IEEE, International Conference on Control Applications, USA .

[14] Yu-Feng Li, Motion, 1999. Control Subject to Nonlinearities and Flexibility (A Overview based on friction and flexibility compensation), Technical report, Department of Machine Design, Royal Institute of Technology, Sweden

[15] Astrom K., Hagglund T., 1995. PID Controllers: Theory, design, tuning. USA. ISBN 1-55617-516-7

Appendices

Appendix 1: MATLAB simulation model with parameters

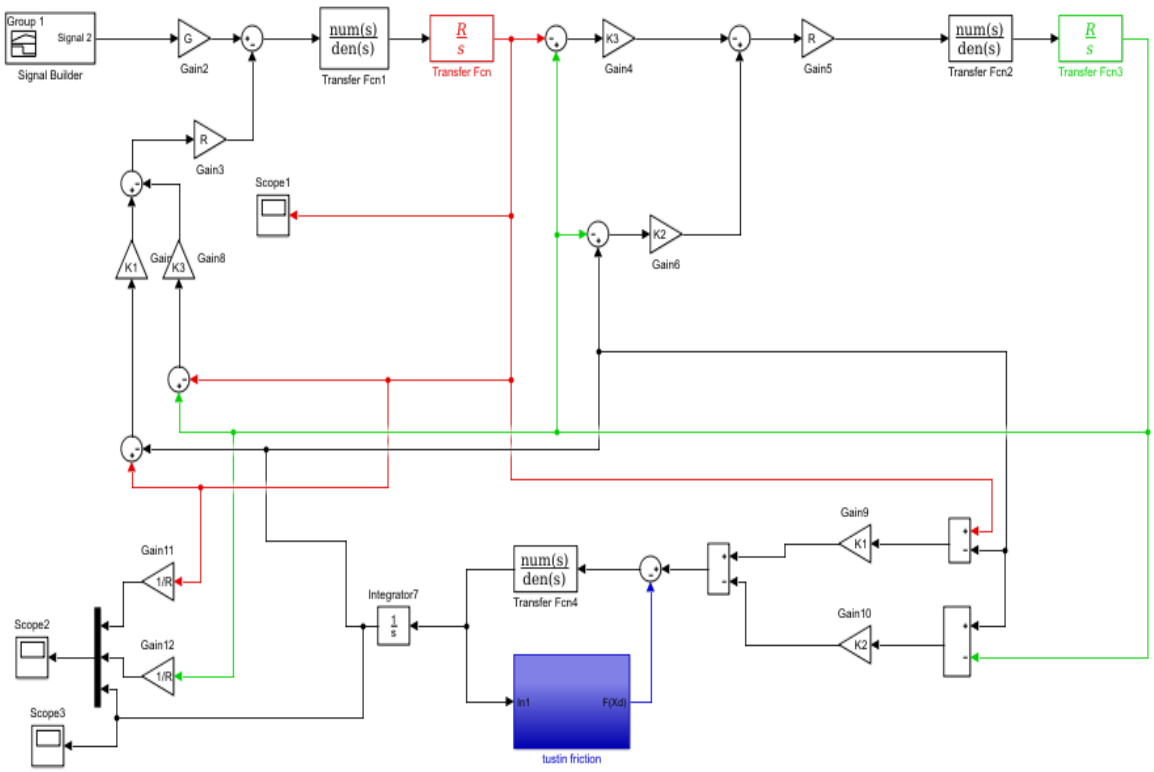

Appendix 2: Specification of the system

PARAMETER	VALUE
DC Voltage source	550v
Stator Resistance	2.875 ohm
q-axis inductance	0.0085H
d-axis inductance	0.0085H
Rotor flux linkage	0.175wb
Moment of inertia,	0.00085kgm^2
Pair of poles	4

Appendix 3: Parameters file

```
% BELT-DRIVE PARAMETERS

clear all;
r1=0.01;
r2=0.02;
rho=7000;
W=0.02;
% the inertia moment of the driving pulley, [kg*m^2]
J1=(0.5*pi*rho*W)*(r2^4-r1^4);
% the inertia moment of the driven pulley, [kg*m^2]
J2 = J1;
% the inertia moment of the motor,
Jm=0.0012;
% the inertia moment of the speed reducer, [kg*m^2]
Jg = 0.1*Jm;
% the mass of the bagasse, [kg]
Mb = 15.1;
% the speed reducer ratio
G = 1;
% the radius of the pulleys, [m]
R = 0.2;
% Belt parameters from manufacturer's data sheet
F=970; % [N]
epsilon=0.267e-2; %[%]
% Belt lenghts [m] at the nominal bagasse position
l3=2.145;
l1=0.74;
l2=1.405;
% Initial values of belt spring constants
% the position dependant elasticity coefficient of the belt 1, [N/m]
K1=F/(epsilon*l1);
% the position dependant elasticity coefficient of the belt 2, [N/m]
K2=F/(epsilon*l2);
% the position dependant elasticity coefficient of the belt 3, [N/m]
K3=F/(epsilon*l3);
%for Tustin's friction model
Fk=35;
Fv=15;
Fs=0;
u0=0.019;
kp_spd=5.11119;
ki_spd=59.34;
kp_id=3.41;
kp_iq =3.41;
ki_id=2327.94;
ki_iq=2327.94;
Tsc=7*2e-6;
ctrl_sat(2)=27.8;
ctrl_sat(1)=-27.8;
nb_p=4;
lambda=0.175;
Ts_vect=2e-6;
h=0.1;
freq_max=20e3;
```